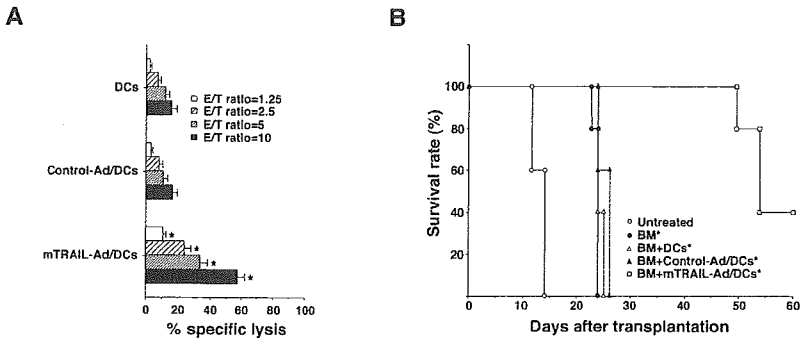

FIGURE 6. Protective effect of TRAIL-transduced murine DCs against leukemia relapse. *A*, The cytotoxicity of uninfected or control-Ad- or mTRAIL-Ad-infected DCs against P815 cells was analyzed by the 4-h ^{51}Cr release assay. Data were expressed as the mean ± SD of triplicate samples, and the values shown are representative of four experiments with similar results. *, $p < 0.01$ compared with uninfected DCs, by Student's paired *t* test. *B*, BALB/c recipient mice were inoculated i.v. with P815 cells (2×10^5) on day −2 and received TBI and i.v. transplantation with C57BL/6 BM cells on day 0. The recipient mice were i.v. injected with or without uninfected or control-Ad- or mTRAIL-Ad-infected BALB/c DCs (5×10^6/mouse) on day 2. Mice were monitored daily for survival. The results are representative of two individual experiments with similar results. *, $p < 0.01$ compared with untreated mice, by Mann-Whitney's *U* test.

Discussion

Gene transfer of immunoregulatory molecules to Ag-presenting DCs provides an attractive approach for the treatment of immunological diseases. Our present findings demonstrate the efficacy of TRAIL gene-transduced DCs for the therapy of lethal acute GVHD and leukemia relapse via elimination of the pathogenic T cells and leukemia cells.

Efficient expression of the introduced gene in target cells is crucial for regulating their function. We showed that the gene transfer of TRAIL into iDCs followed by inflammatory stimulation caused maximal expression of TRAIL. The precise molecular mechanism by which inflammatory stimulation up-regulated the expression of transduced TRAIL gene in DCs remains unknown, but inflammatory stimulation might activate certain transcriptional factors, leading to transactivation of the transduced TRAIL gene. In contrast, mDCs show more potent interaction with Ag-specific T cells than iDCs due to their higher expression of MHC and adhesion/costimulatory molecules. Thus, the maturation of iDCs genetically engineered to express TRAIL by inflammatory stimulation provides advantages for TRAIL expression as well as Ag-specific interaction with T cells.

We showed that human and murine TRAIL-sensitive cell types, including $CD4^+$ T cells primed with allogeneic DCs as well as Jurkat cells and L929 cells, exhibited high expression of DR5, indicating that DR5 is crucial for TRAIL-mediated cytotoxicity. In contrast, analysis of the cell surface expression of TRAIL receptors as well as their transcriptional expression (data not shown) revealed that human and murine DCs showed similar expression levels of these TRAIL receptors. Therefore, suppression of binding of TRAIL to DRs by DcRs may contribute to the low sensitivity of these cell types to TRAIL-mediated cytotoxicity. Collectively, our results suggest that the balance of the expression of DRs and DcRs may determine the sensitivity to TRAIL-mediated cytotoxicity.

The weak suppressive effect of recombinant soluble TRAIL on alloreactive T cell proliferation might be due to a blockage of cell cycle progression as previously reported (6, 7), whereas mDCs genetically modified to express TRAIL could effectively induce apoptosis in alloreactive T cells. Although the precise molecular mechanism underling the difference in the biological function between soluble TRAIL and membrane-bound transduced TRAIL on DCs remains unknown, this phenomenon might reflect the strength of intracellular signaling via DRs. Additional study will be needed to test this possibility.

Although host-matched or -mismatched mTRAIL-transduced DCs may lyse donor-derived T cells that overexpresses mDRs regardless of histocompatibility differences, host-matched mTRAIL-transduced DCs could more effectively lyse host-reactive, donor-derived T cells than host-mismatched, mTRAIL-transduced DCs, because they show more potent reactivity to host-matched, mTRAIL-transduced DCs than host-mismatched, mTRAIL-transduced DCs. Indeed, BALB/c-derived, mTRAIL-Ad/DCs, but not C57BL/6-derived, mTRAIL-Ad/DCs, ameliorated acute GVHD in BALB/c recipients transplanted with C57BL6 BM and spleen cells. Therefore, host-type, TRAIL-transduced DCs are useful for the protection of recipients from lethality induced by acute GVHD in allogeneic BMT.

The expansion of donor-derived $CD4^+$ and $CD8^+$ T cells was markedly suppressed by a single injection of host-type, mTRAIL-transduced DCs. These results suggest that interaction of alloreactive $CD4^+$ and $CD8^+$ T cells with the infused TRAIL-transduced mDCs caused their apoptosis via up-regulation of mDR5, resulting in their selective elimination in vivo. In contrast, donor-derived $CD4^+$ T cells obtained from these protected recipients showed a reduced proliferative response to host-type mDCs. Our results imply that the intracellular signaling events involving TRAIL/DR5 induce not only apoptosis but also functional deficiency in the targeted $CD4^+$ T cells. We also showed that the CTL activity of donor-derived $CD8^+$ T cells was greatly impaired in these protected recipients. Although the precise mechanism remains unclear, the functional impairment of donor-derived $CD4^+$ T cells may contribute to the reduced response of donor-derived $CD8^+$ T cells.

The deletion of donor-derived alloreactive T cells by mTRAIL-transduced DCs can ameliorate acute GVHD, but also may impair their GVL effect. However, our results showed that the TRAIL-transduced DCs could protect BMT recipients from leukemia relapse. This seems likely to be mediated by antileukemic effect of TRAIL expressed on DCs, because the TRAIL-transduced DCs exhibited potent cytotoxic activity in vitro. The ex vivo removal of donor T cell proportions from the marrow graft not only reduced the incidence and severity of acute GVHD, but also increased the risk of leukemia relapse due to lack of GVL effect (19–21). Therefore, our results imply that the use of TRAIL-transduced DCs and T cell-depleted BM inocula might be an alternative strategy for the prevention of acute GVHD and leukemia relapse in human leukemia patients undergoing allogeneic BMT.

The role of TRAIL in hepatic cell death is controversial (29, 30). We observed that a single injection of mTRAIL-Ad/DCs did not induce any apparent liver cytotoxicity in normal mice or recipients of allogeneic BMT (data not shown). Additional study will be needed to determine the safety and potential side effects of TRAIL-transduced DCs in vivo.

In the present study we demonstrated a potent effect of TRAIL-transduced DCs to ameliorate acute GVHD. A similar strategy may be also useful for Ag-specific immunosuppression in allogeneic organ transplantation, autoimmune diseases, and allergic diseases. Studies are now underway to address this possibility.

Acknowledgments

We thank K. Sato, Y. Sato, A. Takeuchi, and M. Yamamoto for excellent assistance.

Disclosures

The authors have no financial conflict of interest.

References

1. Lahm, A., A. Paradisi, D. R. Green, and G. Melino. 2003. Death fold domain interaction in apoptosis. *Cell Death Differ. 10:10.*
2. Smyth, M. J., K. Takeda, Y. Hayakawa, J. J. Peschon, M. R. van den Brink, and H. Yagita. 2003. Nature's TRAIL: on a path to cancer immunotherapy. *Immunity 18:1.*
3. Smyth, M. J., E. Cretney, K. Takeda, R. H. Wiltrout, L. M. Sedger, N. Kayagaki, H. Yagita, and K. Okumura. 2001. Tumor necrosis factor-related apoptosis-inducing ligand (TRAIL) contributes to interferon γ-dependent natural killer cell protection from tumor metastasis. *J. Exp. Med. 193:661.*
4. Takeda, K., Y. Hayakawa, M. J. Smyth, N. Kayagaki, N. Yamaguchi, S. Kakuta, Y. Iwakura, H. Yagita, and K. Okumura. 2001. Involvement of tumor necrosis factor-related apoptosis-inducing ligand in surveillance of tumor metastasis by liver natural killer cells. *Nat. Med. 7:94.*
5. Kayagaki, N., N. Yamaguchi, M. Nakayama, A. Kawasaki, H. Akiba, K. Okumura, and H. Yagita. 1999. Involvement of TNF-related apoptosis-inducing ligand in human $CD4^+$ T cell-mediated cytotoxicity. *J. Immunol. 162:2639.*
6. Song, K., Y. Chen, R. Goke, A. Wilmen, C. Seidel, A. Goke, B. Hilliard, and Y. Chen. 2000. Tumor necrosis factor-related apoptosis-inducing ligand (TRAIL) is an inhibitor of autoimmune inflammation and cell cycle progression. *J. Exp. Med. 191:1095.*
7. Lunemann, J. D., S. Waiczies, S. Ehrlich, U. Wendling, B. Seeger, T. Kamradt, and F. Zipp. 2002. Death ligand TRAIL induces no apoptosis but inhibits activation of human (auto)antigen-specific T cells. *J. Immunol. 168:4881.*
8. Lamhamedi-Cherradi, S. E., S. J. Zheng, K. A. Maguschak, J. Peschon, and Y. H. Chen. 2003. Defective thymocyte apoptosis and accelerated autoimmune diseases in $TRAIL^{-/-}$ mice. *Nat. Immunol. 4:255.*
9. Cretney, E., A. P. Uldrich, S. P. Berzins, A. Strasser, D. I. Godfrey, and M. J. Smyth. 2003. Normal thymocyte negative selection in TRAIL-deficient mice. *J. Exp. Med. 198:491.*
10. Hilliard, B., A. Wilmen, C. Seidel, T. S. Liu, R. Goke, and Y. Chen. 2001. Roles of TNF-related apoptosis-inducing ligand in experimental autoimmune encephalomyelitis. *J. Immunol. 166:1314.*
11. Banchereau, J., F. Briere, C. Caux, J. Davoust, S. Lebecque, Y. J. Liu, B. Pulendra, and K. Palucka. 2000. Immunobiology of dendritic cells. *Annu. Rev. Immunol. 18:767.*
12. Steinman, R. M., and M. C. Nussenzweig. 2002. Avoiding horror autotoxicus: the importance of dendritic cells in peripheral T cell tolerance. *Proc. Natl. Acad. Sci. USA 99:351.*
13. Morelli, A. E., and A. W. Thomson. 2003. Dendritic cells: regulators of alloimmunity and opportunities for tolerance induction. *Immunol. Rev. 196:125.*
14. Matsue, H., K. Matsue, M. Walters, K. Okumura, H. Yagita, and A. Takashima. 1999. Induction of antigen-specific immunosuppression by CD95L cDNA-transfected 'killer' dendritic cells. *Nat. Med. 5:930.*
15. Lu, L., W. C. Lee, T. Takayama, S. Qian, A. Gambotto, P. D. Robbins, and A. W. Thomson. 1999. Genetic engineering of dendritic cells to express immunosuppressive molecules (viral IL-10, TGF-β, and CTLA4Ig). *J. Leukocyte Biol. 66:293.*
16. Morita, Y., J. Yang, R. Gupta. K. Shimizu, E. A. Shelden, J. Endres, J. J. Mule, K. T. McDonagh, and D. A. Fox. 2001. Dendritic cells genetically engineered to express IL-4 inhibit murine collagen-induced arthritis. *J. Clin. Invest. 107:1275.*
17. Liu, Z., X. Xu, H. C. Hsu, A. Tousson, P. A. Yang, Q. Wu, C. Liu, S. Yu, H. G. Zhang, and J. D. Mountz. 2003. CII-DC-AdTRAIL cell gene therapy inhibits infiltration of CII-reactive T cells and CII-induced arthritis. *J. Clin. Invest. 112:1332.*
18. Shlomchik, W. D., M. S. Couzens, C. B. Tang, J. McNiff, M. E. Robert, J. Liu, M. J. Shlomchik, and S. G. Emerson. 1999. Prevention of graft versus host disease by inactivation of host antigen-presenting cells. *Science 285:412.*
19. Tsukada, N., T. Kobata, Y. Aizawa, H. Yagita, and K. Okumura. 1999. Graft-versus-leukemia effect and graft-versus-host disease can be differentiated by cytotoxic mechanisms in a murine model of allogeneic bone marrow transplantation. *Blood 93:2738.*
20. Schmaltz, C., O. Alpdogan, B. J. Kappel, S. J. Muriglan, J. A. Rotolo, J. Ongchin, L. M. Willis, A. S. Greenberg, J. M. Eng, J. M. Crawford, et al. 2002. T cells require TRAIL for optimal graft-versus-tumor activity. *Nat. Med. 8:1433.*
21. Sato, K., N. Yamashita, N. Yamashita, M. Baba, and T. Matsuyama. 2003. Regulatory dendritic cells protect mice from murine acute graft-versus-host disease and leukemia relapse. *Immunity 18:367.*
22. Sato, K., N. Yamashita, M. Baba, and T. Matsuyama. 2003. Modified myeloid dendritic cells act as regulatory dendritic cells to induce anergic and regulatory T cells. *Blood 101:3581.*
23. Kayagaki, N., N. Yamaguchi, M. Nakayama, K. Takeda, H. Akiba, H. Tsutsui, H. Okamura, K. Nakanishi, K. Okumura, and H. Yagita. 1999. Expression and function of TNF-related apoptosis-inducing ligand on murine activated NK cells. *J. Immunol. 163:1906.*
24. Nishimura, N., Y. Nishioka, T. Shinohara, H. Ogawa, S. Yamamoto, K. Tani, and S. Sone. 2001. Novel centrifugal method for simple and highly efficient adenovirus-mediated green fluorescence protein gene transduction into human monocyte-derived dendritic cells. *J. Immunol. Methods 253:113.*
25. Uno, K., T. Inukai, N. Kayagaki, K. Goi, H. Sato, A. Nemoto, K. Takahashi, K. Kagami, N. Yamaguchi, H. Yagita, et al. 2003. TNF-related apoptosis-inducing ligand (TRAIL) frequently induces apoptosis in Philadelphia chromosome-positive leukemia cells. *Blood 101:3658.*
26. Takeda, K., N. Yamaguchi, H. Akiba, Y. Kojima, Y. Hayakawa, J. E. Tanner, T. J. Sayers, N. Seki, K. Okumura, H. Yagita, et al. 2004. Induction of tumor-specific T cell immunity by anti-DR5 antibody therapy. *J. Exp. Med. 199:437.*
27. Fanger, N. A., C. R. Maliszewski, K. Schooley, and T. S. Griffith. 1999. Human dendritic cells mediate cellular apoptosis via tumor necrosis factor-related apoptosis-inducing ligand (TRAIL). *J. Exp. Med. 190:1155.*
28. Yu, Y., S. Liu, W. Wang, W. Song, M. Zhang, W. Zhang, Z. Qin, and X. Cao. 2002. Involvement of tumour necrosis factor-α-related apoptosis-inducing ligand in enhanced cytotoxicity of lipopolysaccharide-stimulated dendritic cells to activated T cells. *Immunology 106:308.*
29. Jo, M., T. H. Kim, D. W. Seol, J. E. Esplen, K. Dorko, T. R. Billiar, and S. C. Strom. 2000. Apoptosis induced in normal human hepatocytes by tumor necrosis factor-related apoptosis-inducing ligand. *Nat. Med. 6:564.*
30. Zheng, S.-J., P. Wang, G. Tsabary, and Y. H. Chen. 2004. Critical roles of TRAIL in hepatic cell death and hepatic inflammation. *J. Clin. Invest. 113:58.*

TCR Engagement Increases Hypoxia-Inducible Factor-1α Protein Synthesis via Rapamycin-Sensitive Pathway under Hypoxic Conditions in Human Peripheral T Cells[1]

Hiroshi Nakamura,* Yuichi Makino,* Kensaku Okamoto,* Lorenz Poellinger,† Kei Ohnuma,* Chikao Morimoto,* and Hirotoshi Tanaka[2]*

Peripheral T cells encounter rapid decrease in oxygen tension because they are activated by Ag recognition and migrate into inflammatory sites or tumors. Activated T cells, therefore, are thought to have such machineries that enable them to adapt to hypoxic conditions and execute immune regulation in situ. We have recently shown that survival of CD3-engaged human peripheral blood T cells is prolonged under hypoxic conditions and hypoxia-inducible factor-1 (HIF-1) and its target gene product adrenomedullin play a critical role for the process. It is also shown that hypoxia alone is not sufficient, but TCR-mediated signal is required for accumulation of HIF-1α in human peripheral T cells. In the present study, we showed that TCR engagement does not influence hypoxia-dependent stabilization but stimulates protein synthesis of HIF-1α, most possibly via PI3K/mammalian target of rapamycin system, and that expression of HIF-1α and its target genes is blocked by treatment with rapamycin. Since some of those gene products, e.g., glucose transporters and phosphoglycerokinase, are considered to be essential for glycolysis and energy production under hypoxic conditions and adequate immune reaction in T cells, this TCR-mediated synthesis of HIF-1α may play a pivotal role in peripheral immune response. Taken together, our results may highlight a novel aspect of downstream signal from Ag recognition by TCR and a unique pharmacological role of rapamycin as well. *The Journal of Immunology,* **2005, 174: 7592–7599.**

Immune cells encounter rapid changes in oxygen tension as they develop and migrate into different compartments of the body (1). Especially peripheral T cells are activated by Ag recognition in inflammatory sites or in tumor, both of which are known to be hypoxic (2). Hypoxic environment is generally considered to be disadvantageous for cellular energy production and survival. It, therefore, appears to be rather paradoxical that activated T cells consume energy to synthesize adhesion molecules and cytokines and perform various functions including adhesion, migration, prolongation of survival and proliferation, cytokine secretion, and cytotoxicity (3). Given this, activated T cells should have such machineries that enable them to adapt for changes in oxygen tension and execute these functions in situ.

The transcription factor hypoxia-inducible factor-1 (HIF-1)[3] is generally believed to be a central regulator of the cellular response to hypoxia (4, 5). HIF-1 induces expression of the genes essential for adaptation to hypoxia including those for erythropoietin, glucose transporters, glycolytic enzymes, and vascular endothelial growth factor (VEGF), eliciting successful homeostatic regulation under hypoxic conditions. Moreover, genetic studies have clearly indicated the essential role of HIF-1α in regulation of inflammation and immune system. For example, genetic disruption of HIF-1α resulted in abnormal B cell development and autoimmunity (6), and selective deletion of HIF-1α gene in granulocytes and macrophages/monocytes was shown to lead to impairment of inflammatory responses such as motility, invasiveness, and bacterial killing of those cells in mice (7).

HIF-1 consists of two distinct basic helix-loop-helix PAS (Per/Arnt/Sim) transcription factors, HIF-1α and HIF-1β. HIF-1α is sensitive to oxygen levels, and, under normoxic conditions, several proline residues are hydroxylated by distinct prolyl hydroxylases and rapidly degraded via ubiquitin-proteasome pathway (4). However, under hypoxic conditions, HIF-1α subunit is stabilized and translocates into the nucleus, thereby homodimerizing with HIF-1β and binding to hypoxia-response element (HRE) DNA sequence on the promoter region of HIF-1 target genes to activate their transcription (8). In addition to this hypoxia-dependent mechanism, recent studies have demonstrated non-hypoxic pathways for regulation of HIF-1α activity (9, 10) and multiple regulatory mechanisms of HIF-1α protein level, may enable cells to adapt to diverse alteration of environments and preserve homeostasis in a tissue-dependent manner. For example, receptor-mediated regulation of HIF-1α expression is thought to be cell and signal specific, and a number of reports have suggested that receptor-mediated factors such as growth factors, hormones, and cytokines induce HIF-1α protein expression through various signalings including PI3K/mammalian target of rapamycin (mTOR) pathway (11–15).

*Division of Clinical Immunology, Advanced Clinical Research Center, Institute of Medical Science, University of Tokyo, Tokyo, Japan; and †Department of Cell and Molecular Biology, Nobel Medical Institute, Karolinska Institute, Stockholm, Sweden

Received for publication October 26, 2004. Accepted for publication March 18, 2005.

The costs of publication of this article were defrayed in part by the payment of page charges. This article must therefore be hereby marked *advertisement* in accordance with 18 U.S.C. Section 1734 solely to indicate this fact.

[1] This work was supported in part by grants from the Ministry of Education, Science, Technology, Sports and Culture, the Ministry of Health, Labor, and Welfare of Japan, the Takeda Science Foundation, the Uehara Memorial Foundation, the Vehicle Racing Commemorative Foundation, Novartis Foundation, and the Cell Science Research Foundation.

[2] Address correspondence and reprint requests to Dr. Hirotoshi Tanaka, Division of Clinical Immunology, Advanced Clinical Research Center, Institute of Medical Science, University of Tokyo, 4-6-1, Shirokanedai, Minato-ku, Tokyo 108-8639, Japan. E-mail address: hirotnk@ims.u-tokyo.ac.jp

[3] Abbreviations used in this paper: HIF-1, hypoxia-inducible factor-1; VEGF, vascular endothelial growth factors; HRE, hypoxia response element; mTOR, mammalian target of rapamycin; ADM, adrenomedullin; GLUT, glucose transporter; PGK1, phosphoglycerate kinase-1; CHX, cycloheximide.

0022-1767/05/$02.00

Rapamycin is an immunosuppressive agent clinically approved for use in kidney transplant patients and additional applications are being considered in autoimmune and chronic inflammatory diseases (16). Rapamycin binds to FK506-binding protein 12, and this complex targets mTOR and inhibits T cell response to IL-2 to progress G_1 to S phase (17). On the other hand, it has been noticed that rapamycin suppresses the growth of certain tumors (18, 19). For example, rapamycin inhibits metastatic tumor growth and angiogenesis in mouse model and this anti-angiogenic activity is shown to link to a decrease in production of VEGF (20). Furthermore, Majumder et al. (21) have clearly indicated that the antitumor effect of rapamycin is, at least in part, mediated by inhibition of mTOR-dependent HIF-1α expression using Akt-dependent prostate intraepithelial neoplasia.

We have recently shown that survival of CD3-engaged human peripheral blood T cells is prolonged under hypoxic conditions, and that HIF-1 and its target gene product adrenomedullin (ADM) play a critical role in the process. Interestingly, it is also shown that hypoxia alone is not sufficient but additional TCR-mediated signal is required for sufficient accumulation of HIF-1α in human peripheral T cells (22). However, underlying mechanisms of TCR-dependent HIF-1α accumulation in human peripheral T cells remain unclear. In the present study, we demonstrated that Ab-mediated TCR engagement does not influence hypoxia-dependent stabilization but stimulates protein synthesis of HIF-1α, most possibly via PI3K/mTOR system, in peripheral blood T cells. Moreover, expression of HIF-1α and its target gene expression was blocked by treatment with rapamycin. Taken together, our results may highlight a novel aspect of downstream signal from Ag recognition by TCR and a unique pharmacological role of rapamycin as well.

Materials and Methods

Abs and reagents

The mAb against human CD3 (UCHT1) was purchased from BD Pharmingen. Anti-human HIF-1α (Ab463) and anti-human HIF-1β Abs were obtained from Abcam. Abs against Akt and phosphorylated Akt at threonine 308 were purchased from Cell Signaling Technologies. Recombinant human IL-2 was obtained from PeproTech and PHA-M from Sigma-Aldrich. Other chemicals were purchased from Sigma-Aldrich unless otherwise specified.

Cell culture and activation of peripheral T cells

Fresh PBMC were prepared from heparinized blood of healthy volunteers by Ficoll-Paque Plus (Amersham Biosciences) density gradient centrifugation and suspended in RPMI 1640 medium (Sigma-Aldrich) supplemented with 10% FBS and antibiotics. Adherent cells were removed by incubation on plastic dishes for 1 h at 37°C, and the rest of the cells were separated on nylon wool columns to obtain T cell rich fraction. For activation, T cell blasts were generated by stimulation of the T cell fraction (1×10^6 cells/ml) with 5 μg/ml PHA-M for 48 h. The mitogen was then washed out, and the cells were maintained in the medium containing 10 ng/ml recombinant human IL-2. For additional experiments, the cells were washed three times with PBS and used as T cells in the present study. CD3 engagement of the cells (1×10^6 cells/ml) was performed in the presence of 10 ng/ml IL-2 on 6-well plates coated with anti-CD3 mAb (5 μg/ml), and exposure of the cells to various oxygen concentrations was conducted as described previously (22).

Western blotting

Immunodetection of HIF-1α protein was performed as described previously (23). Briefly, whole cell extracts of T cells were prepared in lysis buffer consisting of 25 mM HEPES, 100 mM NaCl, 5 mM EDTA, 100 μM orthovanadate, and 0.5% Triton X-100, pH 7.9, followed by centrifugation at 14,000 rpm for 30 min at 4°C. Whole cell extract (60 μg) was separated with SDS-PAGE and electrically transferred onto polyvinylidene fluoride filters. The filters were incubated with anti-HIF-1α Ab at a dilution of 1:1000 in PBS containing 1% nonfat milk at 4°C overnight, followed by anti-mouse Ig-HRP conjugates (Amersham Biosciences) in the same buffer. Immunocomplexes were visualized using ECL as recommended by the manufacturer (Amersham Biosciences).

Northern blotting

Total RNA isolation from human peripheral T cells and Northern blot analysis were performed as described elsewhere (13). In brief, 2×10^7 T cells were stimulated with anti-CD3 Ab under normoxic or hypoxic conditions and harvested. Total RNA was isolated from T cells by guanidine isothiocyanate lysis/phenol chloroform extraction, followed by removal of contaminating DNA, and 10-μg aliquots of RNA were fractionated by electrophoresis in 1.5% agarose 2.2 M formaldehyde gels, transferred to Hybond N membranes (Amersham Biosciences), and hybridized with a ^{32}P-labeled human HIF-1α cDNA probe.

Metabolic labeling

A total of 1×10^7 of T cells were incubated in a 6-well plate with or without 5 μg/ml anti-CD3 Ab. The cells were pretreated with or without MG132 in methionine-free RPMI 1640 medium. [^{35}S]Methionine-cysteine was added to a final concentration of 0.3 mCi/ml, and the cells were pulse labeled for 30 min and then harvested. Whole cell extracts were prepared with RIPA buffer (50 mM Tris-HCl, 150 mM NaCl, 1 mM EDTA, 1% Triton X-100, 0.1% SDS, 0.1% sodium deoxycholate). Cell extract was precleared with protein A-Sepharose for 1 h. Anti-HIF-1α Ab was added to the supernatant and rotated overnight at 4°C. Twenty microliters of 50% slurry of protein A-Sepharose equilibrated with RIPA buffer was added to the mixture, rotated for 2 h at 4°C, pelleted and washed four times with RIPA buffer. Precipitated materials were eluted by boiling in SDS sample buffer. Samples were separated with SDS-PAGE, and the gel was vacuum dried and visualized by autoradiography.

RT-PCR analysis

First strand cDNA was synthesized using 2 μg of DNase-treated total RNA as a template in 20 μl of reaction mixture containing 50 mM Tris-HCl (pH 8.3), 3 mM $MgCl_2$, 10 mM DTT, 75 mM KCl, 1 mM dNTP, 0.1 mM oligo(dT) primer, and 50 U of Superscript II (Invitrogen Life Technologies) at 42°C for 50 min. PCR was conducted in a total volume of 30 μl in a mixture composed of 10 mM Tris-HCl (pH 8.3), 50 mM KCl, 1.5 mM $MgCl_2$, 200 μM dNTP, 0.25 μM each of the sense and antisense primers, and 1 U of ExTaq DNA polymerase (TaKaRa). The amount of cDNA, as judged by the intensity of the amplified β-actin signal, was comparable among the preparations. Amplification by 27 cycles of 94°C for 30 s, 50°C for 30 s, and 72°C for 1 min was performed after 3 min of denaturing of the samples at 94°C and shown to be within linear range or non-saturated conditions for each primers amplification. Identities of the PCR products were confirmed by DNA sequencing. Primer pairs for amplification of each gene are as follows: HIF-1α, sense: 5′- CTGTGATGAGGCTTACCAT CAGC-3′, antisense: 5′-CTCGGCTAGTTAGGGTACACTTC-3′; ADM, sense: 5′-GCGATCCGACTCACCAATAC-3′; antisense: 5′-TGGATCC TGAGTCGAAGTCT-3′; glucose transporter-1 (GLUT-1), sense: 5′-CTT TCTCCAGCCAGCAATGA-3′, antisense: 5′-TGGATCCTGAGTCGAA GTCT-3′; GLUT-3, sense: 5′-GATGCTGGAGAGGTTAAGGT-3′, antisense: 5′- ACTTCCACCCAGAGCAAAGT-3′; phosphoglycerate kinase-1 (PGK1), sense: 5′-CGAGCCAGCCAAAATAGAAGC-3′, antisense: 5′-TCAAACAGAGAAGTGCCAATC-3′; VEGF, sense: 5′-TGCCT

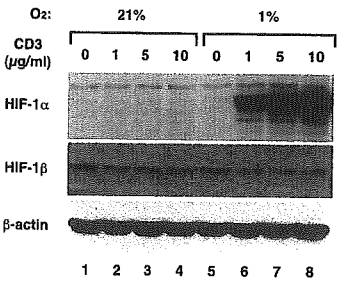

FIGURE 1. TCR engagement-mediated accumulation of HIF-1α protein expression in peripheral T cells. Human peripheral blood T cells were incubated in the absence or presence of increasing concentrations of immobilized anti-CD3 mAb (CD3) for 12 h under 21 or 1% oxygen concentration. Whole cell extracts were prepared and immunoblotting was performed with anti-HIF-1α, HIF-1β, and β-actin Abs as described in *Materials and Methods*.

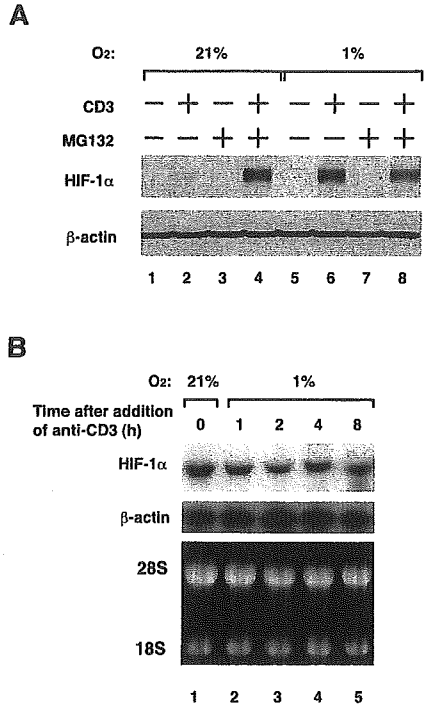

FIGURE 2. Effect of CD3/TCR engagement on protein stability and steady-state level of mRNA of HIF-1α. *A*, Immunoblots for HIF-1α. Human peripheral blood T cells were cultured in the absence or presence of 5 μg/ml immobilized anti-CD3 mAb (CD3) or 5 μM MG132 for 12 h under 21 or 1% oxygen concentration as indicated. Protein levels of HIF-1α and β-actin were determined as described in *Materials and Methods*. *B*, Northern blot analysis for HIF-1α mRNA. Human peripheral blood T cells were cultured in the absence or presence of 5 μg/ml immobilized anti-CD3 mAb under 21 or 1% oxygen concentration for the indicated time periods. After isolation of total RNA, Northern blot for HIF-1α (*top*) or β-actin (*middle*) was performed as described in *Materials and Methods*. As a loading control, ethidium bromide-stained gel was presented in the bottom.

TGCTGCTCTACCTCC-3′, antisense: 5′-TCACCGCCTCGGCTTGT CAC-3′; IL-2, sense: 5′-ATGTACAGGATGCAACTCCTGTCTT-3′; antisense: 5-AGCTGTTTCAGTTCTGTGGCCTTCT-3′; β-actin, sense: 5′-CCTCGCCTTTGCCGATCC-3′, antisense: 5′-GGATCTTCATGAG GTAGTCAGTC-3′.

Transient transfection and luciferase assay

Jurkat T cell line stably expressing constitutive active form of HIF-1α or mock-DNA were grown to confluence in RPMI 1640 medium plus 10% FBS and other supplements. Cells were transfected with plasmid DNA containing promoter-reporter constructs by an electroporation method. Briefly, cells were washed twice with Opti-MEM (Invitrogen Life Technologies) and resuspended in the same medium at a concentration of 2×10^7 cells/ml. Cell suspension was placed in a electroporation cuvette (Gene Pulser; Bio-Rad) followed by adding 5 μg of HRE reporter plasmid DNA. The electroporation was conducted at a capacitance of 950 microfarads and 250 V. After electroporation, the cells were kept on ice for 10 min and resuspended in 10 ml of complete RPMI 1640 medium, and incubated for 12 h at 37°C in 5%. Then cells were further incubated for 36 h in either normoxic or hypoxic conditions. Luciferase enzyme activity was determined using a luminometer (Promega), and relative light units were normalized to the protein amount determined with BCA protein assay reagent according to the manufacturer's instructions (Pierce).

Results

We first analyzed the effect of TCR-mediated signals on protein levels of HIF-1α in human peripheral T cells under hypoxic conditions. For that purpose, human peripheral T cells were treated with various doses of an immobilized mAb against CD3 under normoxic (21%) or hypoxic (1%) conditions and Western blot was performed to determine HIF-1α protein. Under normoxic condition, HIF-1α was not detected even in the presence of relatively high concentration of anti-CD3 mAb. However, under hypoxic condition, TCR/CD3 engagement up-regulated protein expression of HIF-1α in a concentration-dependent manner but did not that of HIF-1β (Fig. 1).

It has recently been reported that HIF-1α expression is regulated at multiple levels including stability/degradation, protein synthesis/translation, and transcription, by a distinct set of upstream signals, dependent on cells or tissues (see introduction). Therefore, we addressed at which level HIF-1α expression is regulated by

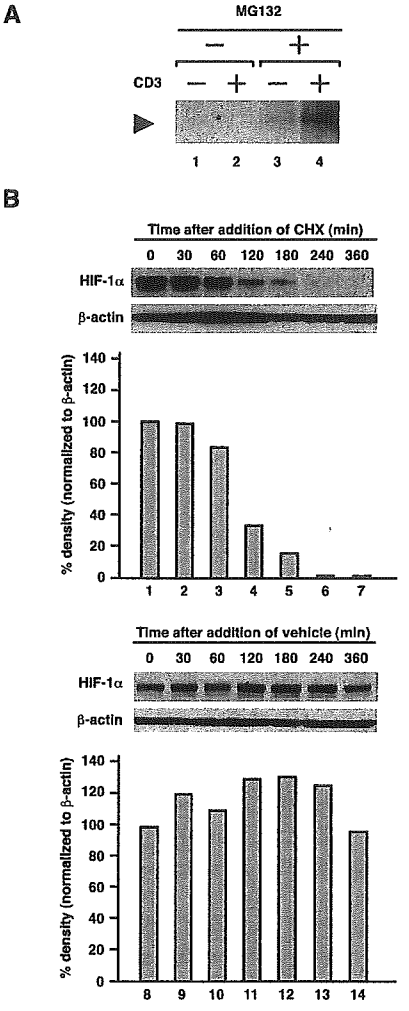

FIGURE 3. TCR/CD3 engagement-dependent HIF-1α protein expression is regulated at the level of protein synthesis. *A*, Metabolic labeling analysis. Serum-starved human peripheral blood T cells were preincubated in the absence or presence of 5 μM MG132 or immobilized anti-CD3 Ab in methionine-free medium for 2 h under normoxic condition as indicated and pulse labeled with 0.3 mCi/ml [^{35}S]methionine-cysteine for 30 min. After isolation of whole cell extracts, HIF-1α was affinity purified by immunoprecipitation and separated by 8% SDS-PAGE as described in *Materials and Methods*. The gel was dried and ^{35}S-labeled HIF-1α protein was detected by autoradiography. *B*, Effect of a protein synthesis inhibitor CHX on HIF-1α protein expression. Human peripheral blood T cells were incubated for 12 h in the absence or presense of 5 μM MG132 and incubated in the presence (*top panel*) or absence (*bottom panel*) of 100 μM CHX for the indicated time periods. HIF-1α and β-actin were analyzed in immunoblots as described in *Materials and Methods*. Density of the bands was measured with NIH IMAGE 1.62 software being normalized to β-actin. Results are shown as relative density (percentage compared with the sample harvested after preincubation with MG132).

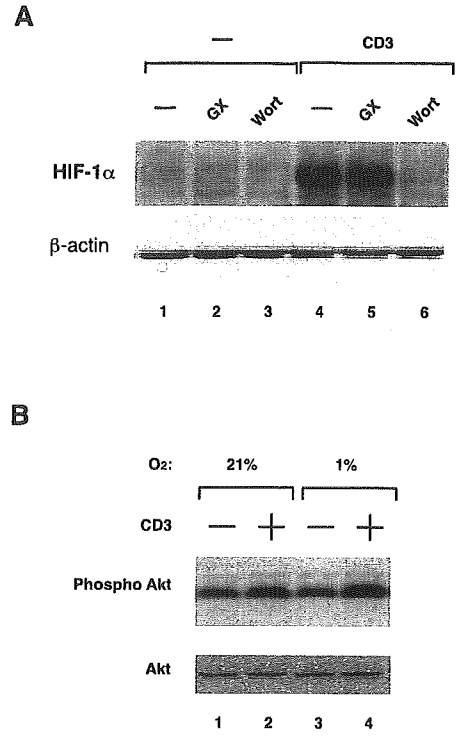

FIGURE 4. Involvement of PI3K activation in TCR/CD3-dependent HIF-1α protein expression. *A*, Immunoblots for HIF-1α. Human peripheral blood T cells were incubated for 12 h in the absence or presence of 10 μM GF109203X (GX), 100 nM wortmannin (Wort), and immobilized anti-CD3 Ab (CD3). HIF-1α and β-actin proteins were detected in immunoblots as described in *Materials and Methods*. *B*, Akt phosphorylation. Human peripheral blood T cells were incubated for 12 h in the absence or presence of immobilized anti-CD3 mAb (CD3) under 21 or 1% oxygen concentration for 12 h. Thr308-phosphorylated form and total Akt protein was detected in immunoblots.

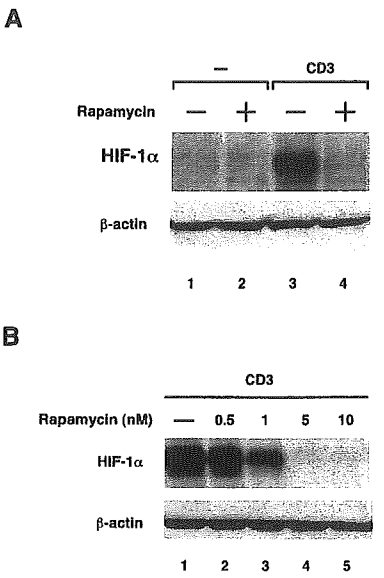

FIGURE 5. Rapamycin inhibits TCR/CD3 engagement-dependent HIF-1α protein expression. Human peripheral blood T cells were incubated for 12 h in the absence or presence of various concentrations of rapamycin (10 nM in *A*, and 0.5, 1, 5, and 10 nM in *B*), or anti-CD3 mAb (CD3) under hypoxic conditions (1% O_2), and HIF-1α or β-actin were detected in immunoblots.

TCR/CD3 ligation in peripheral blood T cells. Concerning protein stability/degradation, treatment of T cells with a proteasome inhibitor MG132 alone failed to restore HIF-1α protein, whereas that in combination with anti-CD3 stimulation successfully restored HIF-1α expression under normoxic condition. Combination of hypoxic treatment and TCR/CD3 ligation up-regulated HIF-1α expression to similar levels, and addition of MG132 did not further increase HIF-1α levels (Fig. 2*A*). These results may indicate that TCR/CD3 engagement does not influence protein stability of HIF-1α and acts via a distinct mechanism concerning the increment of HIF-1α protein accumulation.

Next we tested the effect of TCR ligation on the steady-state level of HIF-1α mRNA in peripheral blood T cells. T cells were stimulated with anti-CD3 mAb for the indicated time period under hypoxic conditions, and cellular contents of HIF-1α mRNA was determined using Northern blot analysis. Expression of HIF-1α mRNA appeared to be unaffected at any time point after application of anti-CD3 mAb (Fig. 2*B*), indicating that alteration in steady-state level of HIF-1α mRNA is unlikely to be responsible for TCR ligation-mediated accumulation of HIF-1α protein in T cells under hypoxic conditions.

Given these results, we examined a role of protein synthesis machinery. For that purpose, we first performed metabolic labeling analysis. Peripheral blood T cells were incubated with anti-CD3 mAb under normoxic conditions in the presence or absence of MG132 then pulse-labeled by means of [^{35}S]methionine-cysteine incorporation followed by immunoprecipitation of HIF-1α. As shown in Fig. 3*A*, ^{35}S-incorporated HIF-1α was clearly detected not in the cells without stimulation but in those treated with anti-CD3 mAb in the presence of MG132 (Fig. 3*A*), indicating that in addition to the inhibition of degradation, an up-regulation of HIF-1α protein synthesis by TCR ligation contributes to HIF-1α protein accumulation. To further confirm this issue, T cells were treated with anti-CD3 mAb in the presence of MG132 under normoxic conditions, then a protein synthesis inhibitor cycloheximide (CHX) was added and the culture was further continued for the indicated time period. HIF-1α protein levels were markedly decreased after addition of CHX, whereas T cells without CHX treatment showed persistent expression of HIF-1α for up to 6 h (Fig. 3*B*). Decrease in HIF-1α protein level started as early as 60 min after treatment with CHX, and HIF-1α protein was hardly detectable after 4 h of treatment with CHX (Fig. 3*B*). These results suggest that detectable HIF-1α protein accumulation requires continuous protein synthesis via CD3/TCR stimulation even when proteasomal degradation is inhibited either under hypoxic conditions or in the presence of MG132.

Because it is shown that HIF-1α protein synthesis is up-regulated mainly via PI3K/mTOR pathway in, for example, cancer cells (see Introduction), we tested the possibility that TCR/CD3 ligation-mediated HIF-1α expression involves PI3K/mTOR pathway as well. For that purpose, we examined the effect of PI3K inhibitor wortmannin, comparing PKC inhibitor GF109203X. It is revealed that not GF109203X but wortmannin completely shuts down HIF-1α expression even under hypoxic condition (Fig. 4*A*). To test the effect of oxygen concentration and TCR/CD3 ligation on PI3K activity, we determined the phosphorylated form of PI3K downstream target Akt. Fig. 4*B* clearly demonstrates that TCR/CD3 ligation does not significantly alter protein levels of Akt but promotes its phosphorylation, and oxygen concentration does not affect the amount of either form of Akt. We next examined the effect of a specific mTOR inhibitor rapamycin on HIF-1α accumulation in peripheral blood T cells. As anticipated, rapamycin completely inhibited the induction of HIF-1α protein expression in anti-CD3-stimulated T cells under hypoxic conditions (Fig. 5*A*).

The inhibitory effect of rapamycin was clearly shown to be concentration dependent (Fig. 5*B*). Therefore, we may conclude that PI3K/mTOR is the major pathway that regulates HIF-1α protein synthesis in TCR-engaged T cells.

To examine the effect of rapamycin on mRNA expression of HIF-1 target genes, T cells were exposed to either hypoxia or normoxia in the absence or presence of anti-CD3 mAb, rapamycin, and MG132 as indicated; then total cellular RNA was prepared, and mRNA expression of HIF-1 target and non-target genes was determined using RT-PCR (Fig. 6). Expression of HIF-1α mRNA was not significantly altered by either of these treatment. In contrast, expression profile of those HIF-1 target genes corresponded to that of HIF-1α protein. That is, combination of anti-CD3 mAb stimulation and either hypoxia or MG132 resulted in significant induction of ADM, GLUT-3, PGK1, VEGF mRNA expression, as well as a robust increase in HIF-1α protein expression. Induction of these mRNAs was inhibited by treatment with rapamycin in accordance with the disappearance of HIF-1α protein expression. Together, these results again indicate that TCR engagement-mediated up-regulation of HIF-1α accumulation and mRNA expression of HIF-1 target genes is rapamycin-sensitive and that protein levels of HIF-1α may, at least in part, determine the levels of mRNA expression of those genes.

We finally addressed the critical requirement of HIF-1α for mRNA expression of those HIF-1 target genes in the experiments with Jurkat cells that express constitutive active mutant of HIF-1α, CA-HIF-1α, which is a chimeric protein consisting of amino acid 1 to 396 of HIF-1α and VP-16 activation domain and escapes from oxygen-dependent degradation (Fig. 7*A*). It should be noted that, in contrast to peripheral blood T cells, hypoxic treatment is sufficient

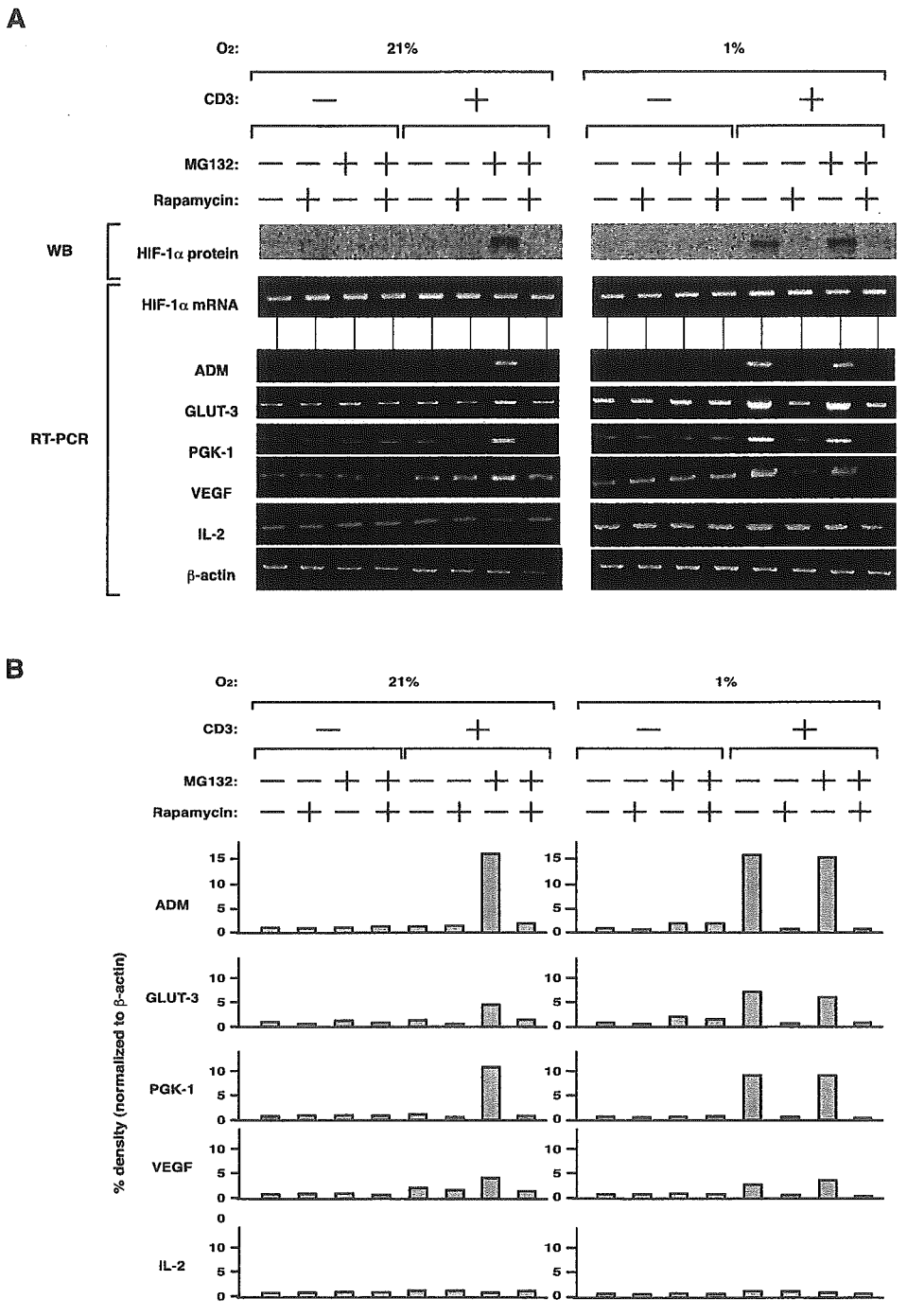

FIGURE 6. Effect of rapamycin on mRNA expression of HIF-1 target and non-target genes. Human peripheral blood T cells were cultured in the absence or presence of 5 μM MG132, 10 nM rapamycin, or 5 μg/ml immobilized anti-CD3 mAb under 21 or 1% oxygen concentration for 18 h. Protein levels of HIF-1α and mRNA levels of HIF-1α and HIF-1 target and non-target genes were determined in immunoblot and RT-PCR, respectively (*A*). Density of the bands was measured with NIH IMAGE 1.62 software being normalized to β-actin and shown in *B*. Results are shown as relative density (percentage compared with the sample without treatment (*left*) or treated with hypoxia alone (*right*)).

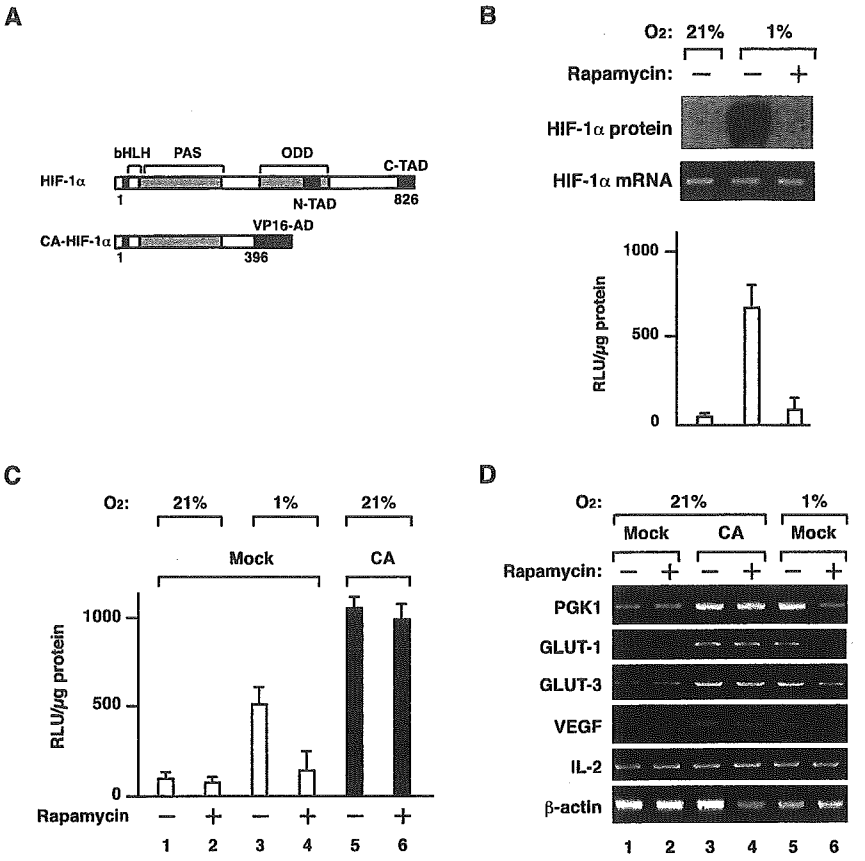

FIGURE 7. Rapamycin acts at the level of protein synthesis of HIF-1α. *A*, Schematic representation of the primary structure of the wild-type HIF-1α and CA-HIF-1α. bHLH, basic helix-loop-helix; PAS, Per/Arnt/Sim homology domain; ODD, oxygen-dependent degradation domain; N-TAD, N-terminal transactivation domain; C-TAD, C-terminal transactivation domain; VP16 AD, VP16 transactivation domain. Numbers depict positions of amino acids. *B*, Hypoxia is sufficient for HIF-1α protein expression in Jurkat cells. Jurkat cells were transfected with HRE luciferase reporter plasmids and cultured under normoxic or hypoxic condition in the presence or absence of rapamycin for 12 h; then whole cell extracts and total RNA were subjected to immunoblots for HIF-1α, luciferase assay, and RT-PCR analysis. Results of luciferase reporter gene assay were shown as relative light units (RLU) normalized to protein content and means ± SD from at least three independent experiments are presented (see *Materials and Methods*). *C*, CA-HIF-1α, bypassing oxygen-dependent degradation, acted as a constitutive transactivator. Mock-transfected (Mock) and CA-HIF-1α-transfected Jurkat cells (CA) were transfected with the HRE luciferase reporter gene and cultured in the presence or absence of 10 nM rapamycin under 21 or 1% oxygen concentration for 24 h. Cells were harvested and luciferase activity was measured. Results were shown as relative light units (RLU) normalized to protein content and means ± SD from at least three independent experiments are presented. *D*, Effect of rapamycin on mRNA expression of HIF-1 target genes in mock- and CA-HIF-1α-transfected Jurkat cells. Mock-transfected (Mock) and CA-HIF-1α-transfected Jurkat cells (CA) were cultured in the presence or absence of 10 nM rapamycin under 21 or 1% oxygen concentration for 24 h. Total RNA was prepared and RT-PCR analysis was performed to monitor mRNA expression of the indicated HIF-1 target genes (PGK,GLUT-1,GLUT-3,VEGF,) or non-HIF-1 target genes (IL-2, β-actin).

for protein expression of HIF-1α and correspondent HRE-driven reporter gene activation in parent Jurkat cells (Fig. 7*B*). Because either treatment with rapamycin (Fig. 7*B*) or serum starvation (data not shown) diminished HIF-1α expression under hypoxic conditions, it is strongly indicated that serum factors are sufficient for protein synthesis of HIF-1α in Jurkat cells in the absence of CD3 engagement as seen in many cancer cells (see introduction). Therefore, to minimize the effect of endogenous HIF-1α, we tested the effect of rapamycin in CA-HIF-1α expressing Jurkat cells under not hypoxic but normoxic conditions (Fig. 7*B*). CA-HIF-1α expressing Jurkat cells showed constitutive activation of the reporter gene expression under normoxic conditions by approximately 2-fold when compared with hypoxic parental or mock-transfected Jurkat cells, confirming that CA-HIF-1α bypassed oxygen-dependent degradation and acted as a constitutive transcriptional activator (Fig. 7, *B* and *C*). The constitutive activation of the reporter gene expression in those cells was not suppressed by rapamycin (Fig. 7*C*), indicating that constitutive active HIF-1α could bypass the inhibitory effect of rapamycin and rapamycin effects upstream of HIF-1α. Moreover, this issue was also reflected in mRNA expression profile of HIF-1α target genes. As shown in Fig. 7*D*, mRNA expression of HIF-1 target genes, PGK1, GLUT-1, GLUT-3, and VEGF in mock-transfected Jurkat cells was increased under hypoxic conditions (*lanes 1* and *5*), and markedly decreased in the presence of rapamycin again as in the case of peripheral blood T cells (*lanes 5* and *6*). In contrast, IL-2 mRNA expression was not significantly influenced in either mock-transfected or CA-HIF1 Jurkat cells. Expression of HIF-1 target genes was increased in CA-HIF-1α expressing Jurkat cells even in normoxic conditions, and the suppressive effect of rapamycin was not observed (*lanes 3* and *4*). Therefore, we may conclude that accumulation of HIF-1α protein in peripheral blood T cells is controlled by dual mechanisms: oxygen-dependent degradation and TCR-mediated synthesis involving PI3K/mTOR, and rapamycin inhibits HIF-1 target gene expression via suppression of HIF-1α synthesis.

Discussion

In this study, we suggested that hypoxia and TCR-mediated signal have distinct roles for HIF-1α expression in peripheral blood T

cells; hypoxia prevents HIF-1α protein degradation as seen in many cells, whereas TCR-mediated signal increases expression of HIF-1α protein, most possibly via enhancement of protein synthesis.

TCR ligation, either with or without CD28 engagement, stimulate PI3K followed by activation of its downstream signals including Akt (24, 25). Together with the fact that PI3K inhibitor wortmannin blocks anti-CD3-mediated HIF-1α expression, it is indicated that activation of PI3K is prerequisite for HIF-1α expression after TCR/CD3 ligation. Moreover, TCR/CD3 ligation increases HIF-1 target genes including glucose transporters and PGK1, which may be essential for supporting energy metabolisms in T cells under hypoxic conditions (26). The Pasteur effect is believed to be the most ancient metabolic adaptation to hypoxia in cells, including decreased oxidative phosphorylation and an increase in anaerobic fermentation (27–29). Because anaerobic fermentation produces far less ATP than oxidative phosphorylation per molecule of glucose, increased activity of the glycolytic pathway is necessary to maintain free ATP levels in the hypoxic cell (28). It has already been reported that HIF-1α and its target genes essentially control the metabolic state and maintain cellular ATP levels via glycolysis during hypoxia (30). Interestingly, Frauwirth et al. (31) reported that, CD3/CD28-mediated activation of PI3K has a distinct role in T cell function, regulating glucose uptake and glycolysis via enhanced expression of, for example, GLUT-1. PI3K activation after ligation of CD3 or CD3/CD28 may, therefore, converge onto the stage of protein translation of HIF-1α to potentiate protein expression of HIF-1α and maintenance of cellular ATP levels and metabolic conditions under hypoxic conditions in situ. Indeed, we have also confirmed that CD3 engagement-mediated increase in HIF-1α expression is further amplified by costimulation via CD28 (data not shown). Collectively, it should be emphasized that TCR signaling diverges into conventionally studied pathways including IL-2 production, and HIF-1-mediated metabolic adaptation, the latter of which is considered to be targeted by rapamycin.

Selective up-regulation of alternatively spliced mRNA isoform of HIF-1α was seen in Ag receptor-activated mice T cells (32). However, this is not the case in human peripheral blood T cells (22). Moreover, it is reported that, in monocyte/macrophage, lipopolysaccharides enhance HIF-1α expression via increased expression of HIF-1α mRNA (15). Hudson et al. (33) showed that rapamycin interferes with HIF-1α activation in hypoxic PC-3 cells by increasing the rate of HIF-1α degradation. Collectively, HIF-1α protein expression might be regulated via distinct mechanisms or pathways in each species, tissue or cell in a spatial- and signal-dependent manner, enabling their rationale adaptation.

Recently, involvement of PI3K/mTOR pathway in HIF-1α synthesis has been described in many cancers. In addition, rapamycin is shown to repress HIF-1α synthesis and expression of HIF-1 target genes including VEGF in these cells via targeting mTOR. Therefore, rapamycin is now considered to act as an antineoplastic agent, as well as an immunosuppressant (18, 34). It appears to be obvious to hypothesize that rapamycin suppresses HIF-1α protein expression in T cells as well. Indeed, we clearly showed that rapamycin dose-dependently decreased HIF-1α expression in CD3-engaged T cells under hypoxic conditions. Moreover, we have shown that rapamycin represses mRNA expression of HIF-1 target genes including PGK1, and GLUTs, which serve as key molecules for glycolysis, as well as that of VEGF. It should be noted that mRNA expression of, for example, IL-2 was reported not to be susceptible to treatment with rapamycin (35). Since the promoter region of the IL-2 gene does not contain HRE, we may conclude that rapamycin rather selectively targets HRE-containing genes and elicits distinct immunosuppression via, at least in part, repression of HIF-1-dependent gene expression (35).

HIF-1α has been shown to be expressed in various inflammatory diseases including Crohn's disease (36), ulcerative colitis (36), and rheumatoid arthritis (22, 37, 38), and expression of those genes is critical for adequate immune response in T cells (see Introduction). TCR-driven activation of PI3K/mTOR and HIF-1α synthesis could be an interesting target for immune modulation, and rapamycin could be one of the exploratory drugs attacking this pathway. On the other hand, classic cytotoxic drugs may have increased risk of secondary neoplasms (39–41). Considering that rapamycin may operate as an antineoplastic agent via, for example, inhibition of VEGF expression in various cancers, it is indicated that rapamycin and its analogues constitute a unique class of immunosuppressive agents from the viewpoint of not only its mechanism of actions but also distinct clinical benefit.

Acknowledgments

We are grateful to all the members of the Morimoto laboratory for fruitful discussion.

Disclosures

The authors have no financial conflict of interest.

References

1. Westermann, J., and U. Bode. 1999. Distribution of activated T cells migrating through the body: a matter of life and death. *Immunol. Today* 20: 302–306.
2. Vaupel, P., O. Thews, D. K. Kelleher, and M. Hoeckel. 1998. Current status of knowledge and critical issues in tumor oxygenation: results from 25 years research in tumor pathophysiology. *Adv. Exp. Med. Biol.* 454: 591–602.
3. Krauss, S., M. D. Brand, and F. Buttgereit. 2001. Signaling takes a breath–new quantitative perspectives on bioenergetics and signal transduction. *Immunity* 15: 497–502.
4. Semenza, G. L. 2004. Hydroxylation of HIF-1: oxygen sensing at the molecular level. *Physiology (Bethesda)* 19: 176–182.
5. Poellinger, L., and R. S. Johnson. 2004. HIF-1 and hypoxic response: the plot thickens. *Curr. Opin. Genet. Dev.* 14: 81–85.
6. Kojima, H., H. Gu, S. Nomura, C. C. Caldwell, T. Kobata, P. Carmeliet, G. L. Semenza, and M. V. Sitkovsky. 2002. Abnormal B lymphocyte development and autoimmunity in hypoxia-inducible factor 1α-deficient chimeric mice. *Proc. Natl. Acad. Sci. USA* 99: 2170–2174.
7. Cramer, T., Y. Yamanishi, B. E. Clausen, I. Forster, R. Pawlinski, N. Mackman, V. H. Haase, R. Jaenisch, M. Corr, V. Nizet, et al. 2003. HIF-1α is essential for myeloid cell-mediated inflammation. *Cell* 112: 645–657.
8. Schofield, C. J., and P. J. Ratcliffe. 2004. Oxygen sensing by HIF hydroxylases. *Nat. Rev. Mol. Cell Biol.* 5: 343–354.
9. Zelzer, E., Y. Levy, C. Kahana, B. Z. Shilo, M. Rubinstein, and B. Cohen. 1998. Insulin induces transcription of target genes through the hypoxia-inducible factor HIF-1α/ARNT. *EMBO J.* 17: 5085–5094.
10. Bilton, R. L., and G. W. Booker. 2003. The subtle side to hypoxia inducible factor (HIFα) regulation. *Eur. J. Biochem.* 270: 791–798.
11. Zhong, H., K. Chiles, D. Feldser, E. Laughner, C. Hanrahan, M. M. Georgescu, J. W. Simons, and G. L. Semenza. 2000. Modulation of hypoxia-inducible factor 1α expression by the epidermal growth factor/phosphatidylinositol 3-kinase/PTEN/AKT/FRAP pathway in human prostate cancer cells: implications for tumor angiogenesis and therapeutics. *Cancer Res.* 60: 1541–1545.
12. Laughner, E., P. Taghavi, K. Chiles, P. C. Mahon, and G. L. Semenza. 2001. HER2 (neu) signaling increases the rate of hypoxia-inducible factor 1α (HIF-1α) synthesis: novel mechanism for HIF-1-mediated vascular endothelial growth factor expression. *Mol. Cell Biol.* 21: 3995–4004.
13. Fukuda, R., K. Hirota, F. Fan, Y. D. Jung, L. M. Ellis, and G. L. Semenza. 2002. Insulin-like growth factor 1 induces hypoxia-inducible factor 1-mediated vascular endothelial growth factor expression, which is dependent on MAP kinase and phosphatidylinositol 3-kinase signaling in colon cancer cells. *J. Biol. Chem.* 277: 38205–38211.
14. Alam, H., E. T. Maizels, Y. Park, S. Ghaey, Z. J. Feiger, N. S. Chandel, and M. Hunzicker-Dunn. 2004. Follicle-stimulating hormone activation of hypoxia-inducible factor-1 by the phosphatidylinositol 3-kinase/AKT/Ras homolog enriched in brain (Rheb)/mammalian target of rapamycin (mTOR) pathway is necessary for induction of select protein markers of follicular differentiation. *J. Biol. Chem.* 279: 19431–19440.
15. Blouin, C. C., E. L. Page, G. M. Soucy, and D. E. Richard. 2004. Hypoxic gene activation by lipopolysaccharide in macrophages: implication of hypoxia-inducible factor 1α. *Blood* 103: 1124–1130.
16. Masri, M. A. 2003. The mosaic of immunosuppressive drugs. *Mol. Immunol.* 39: 1073–1080.
17. Hay, N., and N. Sonenberg. 2004. Upstream and downstream of mTOR. *Genes Dev.* 18: 1926–1945.

18. Guba, M., C. Graeb, K. W. Jauch, and E. K. Geissler. 2004. Pro- and anti-cancer effects of immunosuppressive agents used in organ transplantation. *Transplantation* 77: 1777–1782.
19. Huang, S., and P. J. Houghton. 2003. Targeting mTOR signaling for cancer therapy. *Curr. Opin. Pharmacol.* 3: 371–377.
20. Guba, M., P. von Breitenbuch, M. Steinbauer, G. Koehl, S. Flegel, M. Hornung, C. J. Bruns, C. Zuelke, S. Farkas, M. Anthuber, et al. 2002. Rapamycin inhibits primary and metastatic tumor growth by antiangiogenesis: involvement of vascular endothelial growth factor. *Nat. Med.* 8: 128–135.
21. Majumder, P. K., P. G. Febbo, R. Bikoff, R. Berger, Q. Xue, L. M. McMahon, J. Manola, J. Brugarolas, T. J. McDonnell, T. R. Golub, et al. 2004. mTOR inhibition reverses Akt-dependent prostate intraepithelial neoplasia through regulation of apoptotic and HIF-1-dependent pathways. *Nat. Med.* 10: 594–601.
22. Makino, Y., H. Nakamura, E. Ikeda, K. Ohnuma, K. Yamauchi, Y. Yabe, L. Poellinger, Y. Okada, C. Morimoto, and H. Tanaka. 2003. Hypoxia-inducible factor regulates survival of antigen receptor-driven T cells. *J. Immunol.* 171: 6534–6540.
23. Kodama, T., N. Shimizu, N. Yoshikawa, Y. Makino, R. Ouchida, K. Okamoto, T. Hisada, H. Nakamura, C. Morimoto, and H. Tanaka. 2003. Role of the glucocorticoid receptor for regulation of hypoxia-dependent gene expression. *J. Biol. Chem.* 278: 33384–33391.
24. Okkenhaug, K., and B. Vanhaesebroeck, B. 2003. PI3K in lymphocyte development, differentiation and activation. *Nat. Rev. Immunol.* 3: 317–330.
25. Ward, S. G., and D. A. Cantrell. 2001. Phosphoinositide 3-kinases in T lymphocyte activation. *Curr. Opin. Immunol.* 13: 332–338.
26. MacDonald, H. R., and C. J. Koch. 1977. Energy metabolism and T-cell-mediated cytolysis. I. Synergism between inhibitors of respiration and glycolysis. *J. Exp. Med.* 146: 698–709.
27. Pasteur, L. 1861. Experience et vues nouvelles sur la nature des fermentations. *Comp. Rend. Acad. Sci.* 52: 1260.
28. Stryer, L. 1995. *Biochemistry*, 4th ed, New York.
29. Hardie, D. G. 2000. Metabolic control: a new solution to an old problem. *Curr. Biol.* 10: R757–R759.
30. Seagroves, T. N., H. E. Ryan, H. Lu, B. G. Wouters, M. Knapp, P. Thibault, K. Laderoute, and R. S. Johnson. 2001. Transcription factor HIF-1 is a necessary mediator of the pasteur effect in mammalian cells. *Mol. Cell Biol.* 21: 3436–3444.
31. Frauwirth, K. A., J. L. Riley, M. H. Harris, R. V. Parry, J. C. Rathmell, D. R. Plas, R. L. Elstrom, C. H. June, and C. B. Thompson. 2002. The CD28 signaling pathway regulates glucose metabolism. *Immunity* 16: 769–777.
32. Lukashev, D., C. Caldwell, A. Ohta, P. Chen, and M. Sitkovsky. 2001. Differential regulation of two alternatively spliced isoforms of hypoxia-inducible factor-1α in activated T lymphocytes. *J. Biol. Chem.* 276: 48754–48763.
33. Hudson, C. C., M. Liu, G. G. Chiang, D. M. Otterness, D. C. Loomis, F. Kaper, A. J. Giaccia, and R. T. Abraham. 2002. Regulation of hypoxia-inducible factor 1α expression and function by the mammalian target of rapamycin. *Mol. Cell Biol.* 22: 7004–7014.
34. Hidalgo, M., and E. K. Rowinsky, E. K. 2000. The rapamycin-sensitive signal transduction pathway as a target for cancer therapy. *Oncogene* 19: 6680–6686.
35. Matsue, H., C. Yang, K. Matsue, D. Edelbaum, M. Mummert, and A. Takashima. 2002. Contrasting impacts of immunosuppressive agents (rapamycin, FK506, cyclosporin A, and dexamethasone) on bidirectional dendritic cell-T cell interaction during antigen presentation. *J. Immunol.* 169: 3555–3564.
36. Giatromanolaki, A., E. Sivridis, E. Maltezos, D. Papazoglou, C. Simopoulos, K. C. Gatter, A. L. Harris, and M. I. Koukourakis. 2003. Hypoxia inducible factor 1α and 2α overexpression in inflammatory bowel disease. *J. Clin. Pathol.* 56: 209–213.
37. Giatromanolaki, A., E. Sivridis, E. Maltezos, N. Athanassou, D. Papazoglou, K. C. Gatter, A. L. Harris, and M. I. Koukourakis. 2003. Upregulated hypoxia inducible factor-1alpha and -2alpha pathway in rheumatoid arthritis and osteoarthritis. *Arthritis Res. Ther.* 5: R193–R201.
38. Hollander, A. P., K. P. Corke, A. J. Freemont, and C. E. Lewis. 2001. Expression of hypoxia-inducible factor 1α by macrophages in the rheumatoid synovium: implications for targeting of therapeutic genes to the inflamed joint. *Arthritis Rheum.* 44: 1540–1544.
39. Penn, I. 1998. Occurrence of cancers in immunosuppressed organ transplant recipients. *Clin. Transpl.* 1998: 147–158.
40. Garver, R. I., Jr., G. L. Zorn, X. Wu, D. C. McGiffin, K. R. Young, Jr., and N. B. Pinkard. 1999. Recurrence of bronchioloalveolar carcinoma in transplanted lungs. *N. Engl. J. Med.* 340: 1071–1074.
41. Euvrard, S., C. Ulrich, and N. Lefrancois. 2004. Immunosuppressants and skin cancer in transplant patients: focus on rapamycin. *Dermatol. Surg.* 30: 628–633.

HEXIM1 forms a transcriptionally abortive complex with glucocorticoid receptor without involving 7SK RNA and positive transcription elongation factor b

Noriaki Shimizu*, Rika Ouchida*, Noritada Yoshikawa*, Tetsuya Hisada*, Hajime Watanabe†, Kensaku Okamoto*, Masatoshi Kusuhara‡, Hiroshi Handa§, Chikao Morimoto*, and Hirotoshi Tanaka*¶

*Division of Clinical Immunology and Department of Rheumatology and Allergy, Institute of Medical Science, University of Tokyo, 4-6-1, Shirokanedai, Minato-ku, Tokyo 108-8639, Japan; †Department of Environmental Biology, National Institute for Basic Biology, National Institutes of Natural Science, Okazaki 444-8787, Japan; ‡Internal Medicine I, National Defense Medical College, Tokorozawa 359-8513, Japan; and §Graduate School of Bioscience and Biotechnology, Tokyo Institute of Technology, Yokohama 226-8501, Japan

Edited by Jan-Åke Gustafsson, Karolinska Institute, Huddinge, Sweden, and approved April 28, 2005 (received for review December 30, 2004)

The HEXIM1 protein has been shown to form a protein–RNA complex composed of 7SK small nuclear RNA and positive transcription elongation factor b (P-TEFb), which is composed of cyclin-dependent kinase 9 (CDK9) and cyclin T1, and to inhibit the kinase activity of CDK9, thereby suppressing RNA polymerase II-dependent transcriptional elongation. Here, we biochemically demonstrate that HEXIM1 forms a distinct complex with glucocorticoid receptor (GR) without RNA, CDK9, or cyclin T1. HEXIM1, through its arginine-rich nuclear localization signal, directly associates with the ligand-binding domain of GR. Introduction of HEXIM1 short interfering RNA and adenovirus-mediated exogenous expression of HEXIM1 positively and negatively modulated glucocorticoid-responsive gene activation, respectively. In the nucleus, HEXIM1 was shown to localize in a distinct compartment from that of the p160 coactivator transcriptional intermediary factor 2. Overexpression of HEXIM1 decreased ligand-dependent association between GR and transcriptional intermediary factor 2. Antisense-mediated disruption of 7SK blunted the negative effect of HEXIM1 on arylhydrocarbon receptor-dependent transcription but not on GR-mediated one, indicating that a class of transcription factors are direct targets of HEXIM1. These results indicate that HEXIM1 has dual roles in transcriptional regulation: inhibition of transcriptional elongation dependent on 7SK RNA and positive transcription elongation factor b and interference with the sequence-specific transcription factor GR via a direct protein–protein interaction. Moreover, the fact that the central nuclear localization signal of HEXIM1 is essential for both of these actions may argue the crosstalk of these functions.

nuclear receptor | RNA-binding protein | ribonucleoprotein | steroid | nuclear localization signal

Transcription is a complex multistep process that relies on highly coordinated actions of a number of cis- and trans-acting elements (1–3). RNA polymerase II (RNAP II), as the central player in transcription of class II genes, carries out a series of events that include promoter binding, transcription initiation, promoter escape, transcription elongation, and transcription termination. During transcription by RNAP II, phosphorylation of the C-terminal domain of the largest subunit of RNAP II by positive transcription elongation factor b (P-TEFb), which is composed of cyclin-dependent kinase 9 (CDK9) and cyclin T1, is crucial for the transition from the abortive to the productive phase of transcriptional elongation, leading to the generation of full-length RNA transcripts. P-TEFb has been shown to lose its ability to phosphorylate the C-terminal domain when associated with 7SK RNA, a 330-nt small nuclear RNA (4–6).

HEXIM1 was first identified as a protein whose expression is induced in vascular smooth muscle cells (VSMC) in response to hexamethylene bisacetamide (HMBA) treatment (7, 8). The HEXIM1 protein consists of 359 amino acids and is tentatively divided into three regions: an N-terminal proline-rich region (amino acids 1–149), a lysine-arginine rich central nuclear localization signal (NLS)-like region (amino acids 150–177), and a C-terminal acidic region enriched in aspartic and glutamic acid residues (amino acids 178–359) (8). Recently, HEXIM1 was shown to bind 7SK via the NLS, which is considered to be an arginine-rich RNA-binding motif, to form a complex with P-TEFb and to potently and specifically inhibit the kinase and transcriptional activities of P-TEFb (9–12). Roughly half of nuclear P-TEFb in HeLa cells is considered to be sequestered in an inactive state with 7SK and HEXIM1. However, this population of P-TEFb can be rapidly dissociated from 7SK and HEXIM1 upon various treatment of cells, some of which in turn cause the stimulation of C-terminal domain phosphorylation and global increase in RNA and protein synthesis (9, 10, 13, 14). It is therefore of particular importance to address how association of HEXIM1 with 7SK and P-TEFb is controlled. On the contrary, HEXIM1 appears to be in large excess over P-TEFb (11). Moreover, it has recently been reported that HEXIM1 might interact with cellular factors other than 7SK/P-TEFb and perform distinct functions (15). Interestingly, a hypothetical protein gene located in a locus adjacent to that of HEXIM1 has a great sequence similarity to HEXIM1. This protein, named HEXIM2, was recently shown to be expressed in testes and to have an elongation-suppressive function as well (16, 17). For further understanding of the role of HEXIMs in transcriptional regulation and gene expression, it is therefore essential to identify partner factors of HEXIMs.

In the present study, we demonstrate that HEXIM1 forms a distinct complex with the glucocorticoid receptor (GR) in an RNA-independent fashion. GR is a classical member of the nuclear receptor superfamily and has a modular structure consisting of the N-terminal transactivating domain [also termed activation function-1 (AF1)], the central DNA-binding domain (DBD), and the C-terminal ligand-binding domain (LBD), and AF2 at the C terminus (18, 19). It is believed that, upon ligand binding, GR translocates into the nucleus and binds to a target DNA sequence, thereby activating transcription via complex interplay with coactivators, mediators, and target DNA (18, 19). HEXIM1, through its arginine-rich NLS, directly associates with the GR LBD and appears to interfere with productive commu-

This paper was submitted directly (Track II) to the PNAS office.

Abbreviations: GR, glucocorticoid receptor; DBD, DNA-binding domain; LBD, ligand binding domain; P-TEFb, positive transcription elongation factor b; NLS, nuclear localization signal; AhR, arylhydrocarbon receptor; VSMC, vascular smooth muscle cells; HMBA, hexamethylene bisacetamide; TIF2, transcriptional intermediary factor 2; CDK9, cyclin-dependent kinase 9; AF1, activation function-1; DEX, dexamethasone.

¶To whom correspondence should be addressed. E-mail: hirotnk@ims.u-tokyo.ac.jp.

nication of GR with the p160 coactivator transcriptional intermediary factor 2 (TIF2). These results indicate that HEXIM1 has dual roles in transcriptional regulation by means of a single arginine-rich domain: inhibition of transcriptional elongation dependent on 7SK RNA and P-TEFb and interference with GR by a direct protein–protein interaction.

Materials and Methods

Recombinant DNA, Antibodies, and Cells. Expression plasmids for FLAG-tagged and GST-fused wild-type and mutant HEXIM1 were described in ref. 8. pGEX/hHEXIM1/Δ150–177+SV, pGEX/hHEXIM1/150–180, pCMX/6His-GR, and its mutants were generated by cloning appropriate PCR fragments into pGEX6P-3 (Amersham Biosciences) or pCMX (20). Expression plasmids for double-stranded hairpin RNAs were constructed from pSilencer3.1-H1 neo (Ambion, Austin, TX). The target sequence used was 5′-gaagaagcggcattggaaa-3′ for HEXIM1. Recombinant adenovirus encoding FLAG- and 6His-HEXIM1 (AdCALNL/FHhHEXIM1) was generated by using an Adenovirus Cre/loxP-regulated Expression Vector set (TaKaRa). The following antibodies were used in this study: GR, TIF2 (catalog nos. 611227 and 610985, respectively, BD Transduction Laboratories), CDK9, cyclinT1, CBP (catalog nos. sc-484G, sc-8127, and sc-369, respectively, Santa Cruz Biotechnology), FLAG, α-actinin (catalog nos. F3165 and A5044, respectively, Sigma), arylhydrocarbon receptor (AhR; catalog no. SA-210, Biomol, Plymouth Meeting, PA), and HEXIM1 (8). HeLa, COS7, and HepG2 cells were obtained from RIKEN Cell Bank (Tsukuba, Japan) and cultured in DMEM (Sigma) supplemented with steroid-stripped 10% FBS (21). Human VSMC were obtained from Kurabo (Osaka, Japan) and maintained as described in ref. 8.

Transfection and Luciferase Assay. Cells (1.5×10^5) were transfected in six-well plates with 500 ng of glucocorticoid-responsive luciferase reporter plasmid (GRE-Luc) or xenobiotic-responsive luciferase reporter plasmid using TransIt-LT1 (Panvera, Madison, WI) (22). After treatment with dexamethasone (DEX) (Sigma) or 3-methylchoranthrene (Sigma) for 24 h, cellular luciferase activity was measured by using a luciferase assay system (Promega). For cotransfection assay with plasmids and antisense 7SK deoxyoligonucleotide, Lipofectamine reagent and Plus reagent (Invitrogen) were used. The deoxyoligonucleotide sequences used were 5′-ccttgagagcttgtttggagg-3′ for antisense 7SK and 5′-cgtcgatgtgatgctgtgtga-3′ for scrambled deoxyoligonucleotide (14).

Affinity Purification and Mass Spectrometry. Bacterially expressed GST-HEXIM1 proteins were immobilized onto glutathione Sepharose 4B resin (Amersham Biosciences). HeLa cell nuclear extracts prepared as described in ref. 23 were incubated with the affinity beads for 1.5 h at 4°C and washed with binding buffer (10 mM Hepes, pH 7.9/10% glycerol/50 mM KCl/6 mM $MgCl_2$/0.1 mM EDTA/0.5 mM DTT/0.5 mM PMSF/0.1% Nonidet P-40). The bound proteins were eluted with elution buffer (10 mM Hepes, pH 7.9/10% glycerol/1 M NaCl/0.1 mM EDTA/0.5 mM DTT/0.5 mM PMSF/0.1% Nonidet P-40) and separated by 5–20% SDS/PAGE, and the amino acid sequence was determined by mass spectrometry as described in ref. 24.

Indirect Immunofluorescence. Cells were plated on coverslips, fixed in 3.7% paraformaldehyde for 20 min at room temperature, permeabilized with 0.1% Triton X-100 in PBS for 15 min, and incubated with blocking buffer (3% BSA/0.1% Triton X-100 in PBS) for 1 h. Cells were incubated for 1 h with primary antibodies and stained with Alexa Fluor 594- or 488-conjugated secondary antibodies (Molecular Probes). Cellular fluorescence was analyzed with Olympus laser scanning confocal microscopy. For digital image analysis, Olympus FLUOVIEW software was used as described in ref. 25.

GST Pull-Down Assays and Immunoprecipitations. 6His-GR and its mutants were *in vitro*-translated with [^{35}S]methionine by using TNT Coupled Reticulocyte Lysate systems (Promega) and incubated for 1.5 h with GST-HEXIM1 immobilized beads. Bound proteins were eluted with sample buffer, separated by SDS/PAGE, and detected by fluorography. For immunoprecipitation, HeLa cell whole-cell extracts (500 μg) were prepared in radioimmunoprecipitation assay buffer (10 mM Tris, pH 7.9/150 mM NaCl/0.1% SDS/1% Triton X-100/1% deoxycholate/1 mM DTT/1 mM PMSF), incubated with 5 μg of anti-HEXIM1 or anti-CDK9 antibody for 1.5 h with or without RNase A, and incubated with protein A-Sepharose (Amersham Biosciences) for 1.5 h. HeLa cell nuclear extracts (200 μg) were prepared as described in ref. 26, incubated with 1 μg of anti-TIF2 antibody for 6 h in immunoprecipitation buffer (20 mM Hepes, pH 7.9/50 mM NaCl/1 mM EDTA/1 mM EGTA/0.1% Nonidet P-40/1 mM DTT/1 mM PMSF/10 μM DEX), and incubated with Protein G-Sepharose (Amersham Biosciences) for 1.5 h. Bound proteins were resolved by SDS/PAGE followed by Western blotting.

RT-PCR and DNA Microarray. Reverse transcription was performed by using SuperScript II (Invitrogen). Specific primers for PCR are described elsewhere (8, 27–29). Total RNA of HepG2 cells was prepared as recommended by Affymetrix. Samples were run by using a GeneChip Human Genome Focus Array (Affymetrix, Santa Clara, CA) comprising 8,746 probe sets representing ≈8,400 human genes. Genes whose expression was significantly detected at any time point were considered to be valid for further analysis, and 5,288 genes were analyzed by using GENECHIP software (Affymetrix) as described in ref. 30.

Results

Complex Formation of HEXIM1 with GR Independent of RNA and P-TEFb. HEXIM1-binding proteins were affinity-purified by using GST-HEXIM1 and identified with mass spectrometry. In the absence of treatment with RNase A, HEXIM1 bound numerous proteins participating in RNA metabolism, probably because of its RNA-binding property (data not shown). In clear contrast, in the presence of an excess of RNase A, we detected a single HEXIM1-binding protein with a molecular weight of 94 kDa (Fig. 1*A*). Mass spectrometric analysis revealed that the protein is GR. Western blot analysis showed that eluates from HEXIM1 affinity beads contained CDK9 and cyclin T1, both of which were diminished in the presence of RNase A (Fig. 1*B*). In contrast, RNase A did not affect the interaction between HEXIM1 and GR (Fig. 1*B*). Immunoprecipitation of HeLa whole-cell extracts with anti-HEXIM1 antibody demonstrated that HEXIM1 forms distinct complexes with P-TEFb and GR in RNA-dependent and -independent manners, respectively (Fig. 1*C*). Because samples immunoprecipitated from the extracts with anti-CDK9 antibody contained HEXIM1 but not GR (Fig. 1*D*), we concluded that HEXIM1 forms at least two protein complexes, one involving P-TEFb and 7SK and the other containing GR. We also concluded that the interaction between HEXIM1 and GR does not require RNA.

HEXIM1 Negatively Modulates Glucocorticoid-Mediated Gene Expression. Adenovirus-mediated overexpression of HEXIM1 in HepG2 cells decreased DEX-induced mRNA expression of endogenous glucocorticoid-regulated genes without significant alteration in GR protein levels in whole-cell extracts (Fig. 2*A*). DNA microarray analysis revealed that expression of 2.5% of the 5,288 annotated genes was repressed by the exogenous FLAG-HEXIM1, possibly because of the inhibition of P-TEFb. Con-

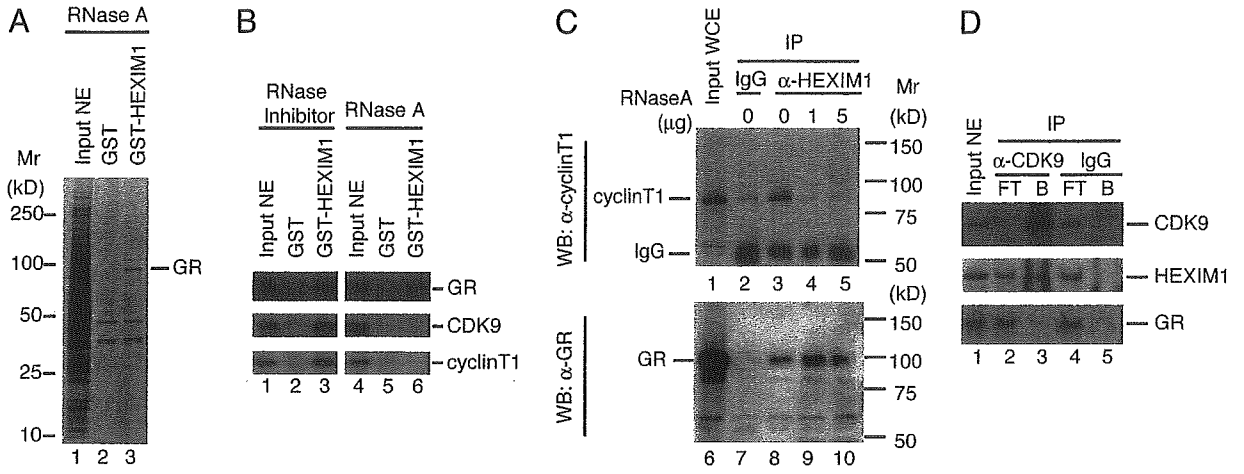

Fig. 1. HEXIM1 forms a distinct complex with GR independent of RNA and P-TEFb. (*A* and *B*) Identification of GR as a HEXIM1-binding protein. Nuclear extracts (NE) from HeLa cells were incubated with GST or GST-HEXIM1 immobilized beads. Bound fractions were analyzed with SDS/PAGE followed by silver staining (*A*) and analyzed on Western blots (WB) (*B*). (*C* and *D*) HEXIM1-GR complex does not contain 7SK RNA, CDK9, or cyclin T1. Whole-cell extracts (WCE) (*C*) or nuclear extracts (*D*) from HeLa cells were immunoprecipitated with anti-HEXIM1 (*C*) or anti-CDK9 (*D*) antibodies in the absence or presence of RNase A. Immunocomplexes were analyzed on Western blots as indicated. IP, immunoprecipitation; FT, flow through; B, bound.

cerning glucocorticoid-regulated genes, 135 genes (2.6% of total) were positively regulated by DEX, and the induction responses of 125 genes (92.6% of 135 genes) were canceled in the presence of exogenous FLAG-HEXIM1 (Fig. 2*B*; see also Table 1, which is published as supporting information on the PNAS web site). Short interfering RNA-mediated knockdown of HEXIM1 did not influence total amounts of GR (data not shown) but enhanced GR-dependent reporter gene expression, which was again canceled by exogenous expression of FLAG-HEXIM1 (Fig. 2*C*). These results indicate the negative regulatory role of HEXIM1 in GR-mediated transcription. In concert with this idea, treatment of VSMC with HMBA, which resulted in enhancement of HEXIM1 protein expression (8), decreased GR-dependent transcription (Fig. 2*D*).

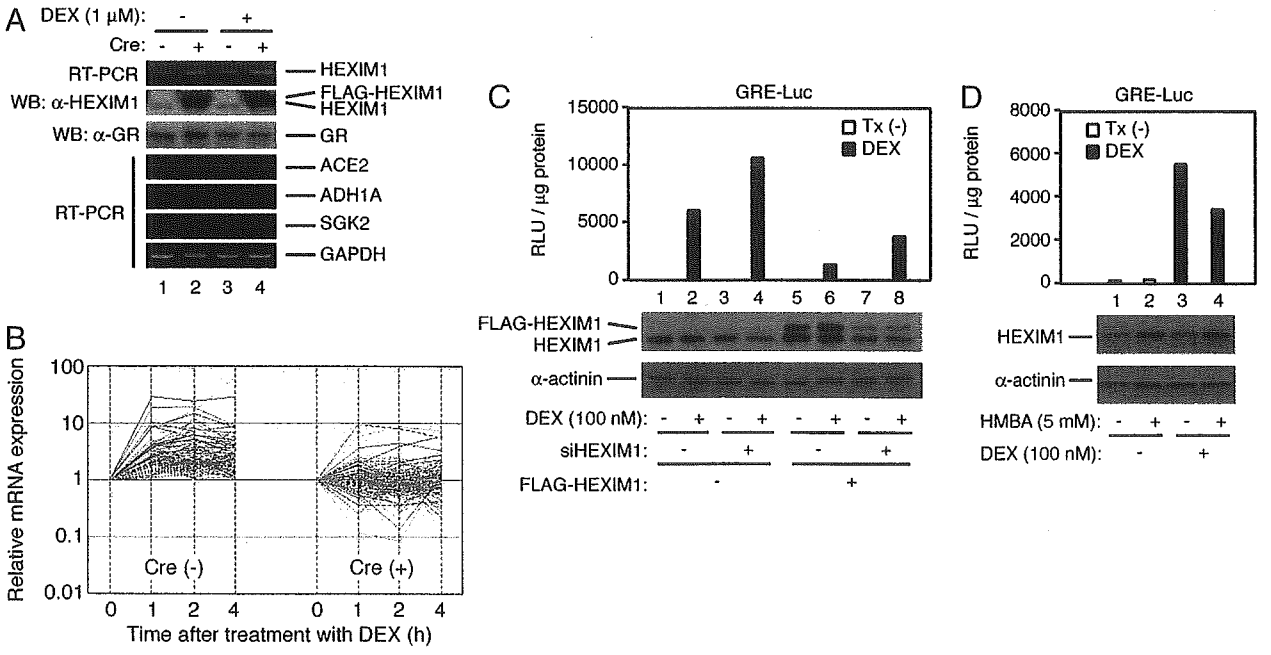

Fig. 2. Effects of HEXIM1 on glucocorticoid-mediated gene expression. (*A*) HepG2 cells were infected with a recombinant adenovirus carrying loxP-flanked FLAG-HEXIM1 cDNA (AdCALNL/FHhHEXIM1; multiplicity of infection = 30) alone (Cre −) or along with a recombinant adenovirus expressing Cre recombinase (Cre +). After a 2-h treatment with 1 μM DEX, mRNA and protein expression levels were analyzed with RT-PCR and Western blots (WB), respectively. ACE2, angiotensin I converting enzyme 2; ADH1A, alcohol dehydrogenase 1A; SGK2, serum/glucocorticoid-regulated kinase 2. (*B*) HepG2 cells were infected with these recombinant adenoviruses and cultured in the presence of 1 μM DEX for 1, 2, or 4 h, and total RNA was isolated and subjected to DNA microarray analysis. Genes whose mRNA expression was increased >2-fold by DEX alone were selected, and their relative mRNA expression levels compared with vehicle-treated cells (0 h) were plotted versus time after treatment with DEX. (*C*) HeLa cells were cotransfected with GRE-Luc, expression plasmids for FLAG-HEXIM1 (FLAG-HEXIM1 +) or empty vector (FLAG-HEXIM1 −), and short interfering RNA against HEXIM1 (siHEXIM1 +) or control vector (siHEXIM1 −), as indicated. After 24 h of treatment with 100 nM DEX, whole-cell extracts were prepared and subjected to luciferase assay and Western blots. (*D*) Human VSMC were transfected with GRE-Luc and cultured in the presence or absence of 5 mM HMBA for 12 h. After 24 h of treatment with 100 nM DEX, whole-cell extracts were prepared and subjected to luciferase assay and Western blots. Tx, treatment; RLU, relative light units.

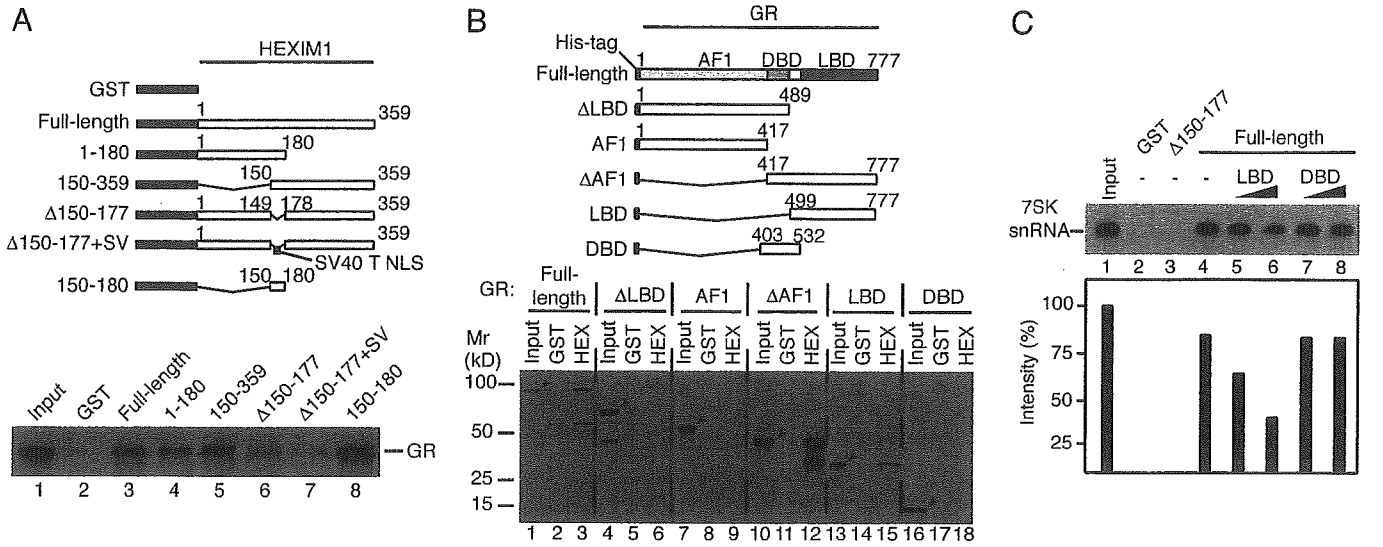

Fig. 3. HEXIM1 directly interacts with GR. (*A* and *B*) GST or GST-fused HEXIM1 mutants were immobilized on glutathione Sepharose beads and incubated with *in vitro*-translated ^{35}S-labeled GR or its mutants, and bound GR was analyzed with SDS/PAGE followed by fluorography. SV40, simian virus 40. (*C*) Four picomoles of GST or GST-fused HEXIM1 mutants were immobilized on glutathione Sepharose beads and incubated with ^{32}P-labeled *in vitro*-transcribed 7SK (lane 1) in the absence or presence of 12 pmol (lanes 5 and 7) or 60 pmol (lanes 6 and 8) of bacterially expressed 6His-GR LBD or DBD as indicated. Bound RNA was analyzed with denaturing PAGE followed by autoradiography. The radioactivity of each band quantified by using Fuji Film BAS2000 image analyzer is shown.

7SK-Binding Domain of HEXIM1 Directly Interacts with GR LBD in a Ligand-Independent Manner. Bacterially expressed GST-HEXIM1 and its various mutants were tested for the interaction with [^{35}S]methionine-labeled *in vitro*-translated full-length GR. Deletion of either N- or C-terminal part of HEXIM1 did not affect binding to GR. However, deletion of the central NLS or its replacement with the simian virus 40 large T-antigen NLS abolished GR binding, and the HEXIM1 NLS alone could strongly bind GR (Fig. 3*A*), indicating that a mere cluster of basic amino acids acting as an NLS is not sufficient and that the native HEXIM1 NLS region is required for binding GR. Next, to identify a HEXIM1-binding domain of GR, bacterially expressed GST-HEXIM1 was immobilized, and *in vitro*-translated 6His-GR or its mutants were applied in the absence of ligand. Either full-length GR, AF1-deleted GR, or the LBD alone could still bind HEXIM1. However, neither AF1 nor DBD was trapped by HEXIM1. Moreover, deletion of the LBD from GR abolished HEXIM1 binding ability, indicating critical requirement of the LBD (Fig. 3*B*). In excellent agreement with this finding, *in vitro* binding of 7SK to HEXIM1 was specifically inhibited by the GR LBD (Fig. 3*C*). Because we obtained similar sets of results when DEX was included in the reactions (data not shown), it is suggested that classical agonists are not critical for the GR–HEXIM1 interaction.

HEXIM1 Interferes with the Interaction Between GR and TIF2. Immunofluorescent analysis revealed that endogenous HEXIM1 constitutively localizes to discrete spots in the nucleus and that ligand-bound GR partially overlaps with HEXIM1 or TIF2 in HeLa cells (Fig. 4*A*). Because HEXIM1 barely colocalized with TIF2 (Fig. 4*A*), we hypothesized that HEXIM1 may compete with TIF2 for binding to GR in a DEX-treated cell nucleus. When HEXIM1 was overexpressed, exogenous expression of TIF2 did not efficiently restore transactivational function of GR (Fig. 4*B*). Moreover, immunoprecipitation of HeLa cell extracts with anti-TIF2 antibody recovered GR but not HEXIM1, and overexpression of HEXIM1 reduced complex formation between GR and TIF2 without significant alteration in the levels of TIF2 (Fig. 4*C*). These results suggest that increase in cellular HEXIM1 down-modulates GR association with TIF2.

Transcription Factor Selectivity of HEXIM1. We next tested the effects of HEXIM1 on AhR, because AhR has been shown to rely on P-TEFb and coactivators, including TIF2, for transcriptional regulation (31, 32). AhR does not directly bind HEXIM1 (data not shown). In HepG2 cell nuclear extracts, adenovirus-mediated overexpression of HEXIM1 did not influence protein levels of either GR or AhR (see Fig. 6, which is published as supporting information on the PNAS web site), and respective ligands increased nuclear fractions of GR and AhR. Transient introduction of antisense deoxyoligonucleotide of 7SK (AS7SK) for disruption of endogenous 7SK (14) resulted in a ≈2.5-fold activation of reporter genes driven by either AhR or GR, indicating the liberation of P-TEFb from 7SK and HEXIM1 to enhance P-TEFb kinase activity. Transactivational activity of AhR and GR was suppressed by HEXIM1 in a dose-dependent manner in the absence of AS7SK. As expected, AS7SK-mediated disruption of 7SK resulted in extinction of HEXIM1 inhibition of AhR. In clear contrast, introduction of AS7SK did not affect the inhibitory effect of HEXIM1 on GR-mediated transcription (Fig. 5), strongly supporting the notion that HEXIM1 suppresses GR-mediated transcription not only through the inhibition of P-TEFb but also by a distinct mechanism that does not involve 7SK. Together, we propose that HEXIM1, by directly binding with GR, may play a distinct role in transcriptional regulation.

Discussion

At this moment, the precise physiological function of HEXIM1 remains unknown. However, genetic disruption of the CLP-1 gene, which is a mouse homologue of HEXIM1, is reported to result in embryonic lethality with marked cardiac hypertrophy (33). Moreover, it is separately shown that hyperactivation of P-TEFb in cardiac myocytes produces cardiac hypertrophy (34). It is therefore likely that HEXIM1 plays an important role in cardiac development and disease pathogenesis. On the other hand, it has been shown that intracellular levels of HEXIM1 are variable and inducible (7, 8). We showed that treatment of VSMC with HMBA resulted in an increase of HEXIM1 expression and a concomitant decrease of GR-activated transcription (8) (see also Fig. 2*D*). Although the role of glucocorticoids in VSMC remains to be clarified, it is likely that

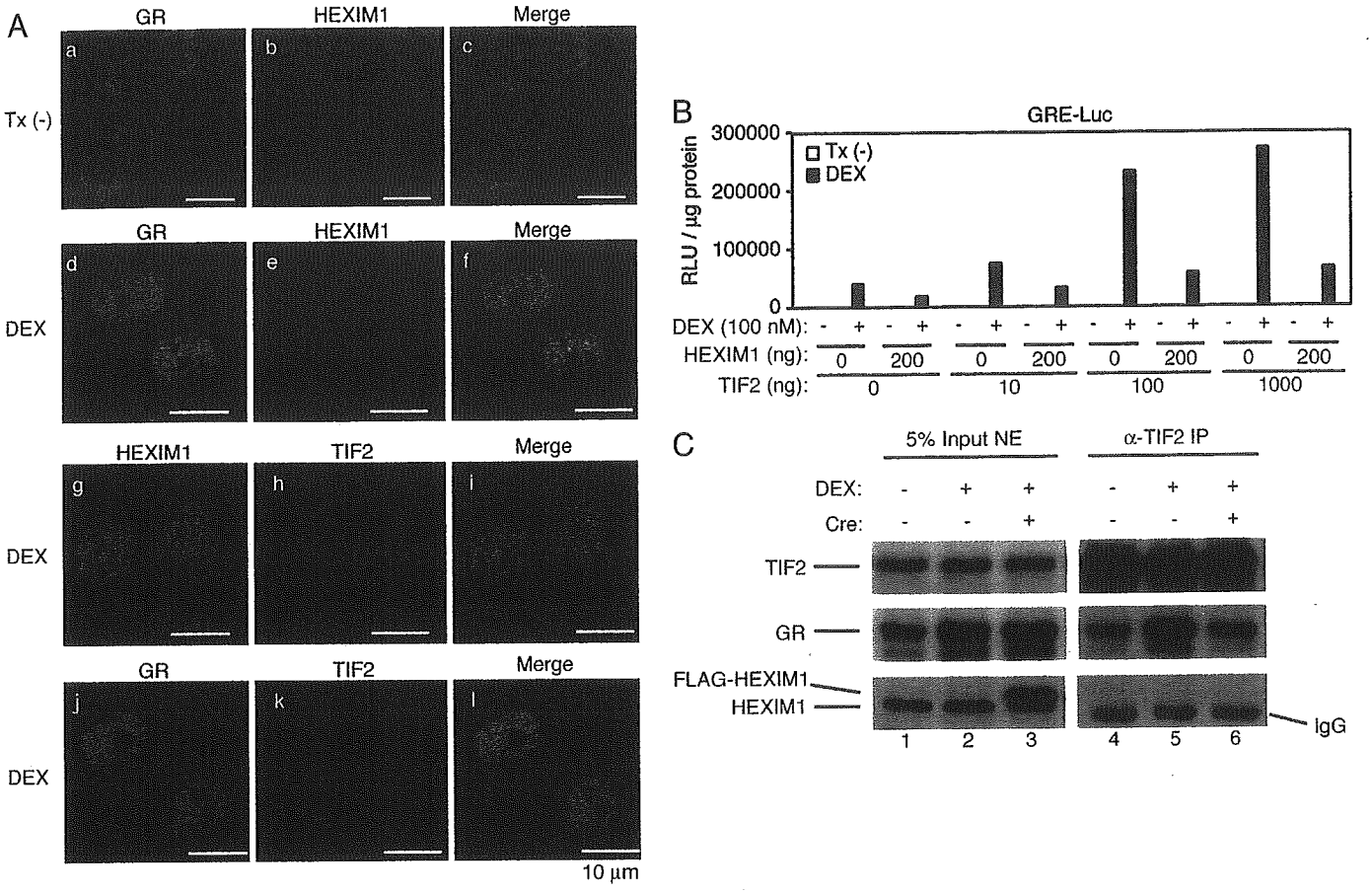

Fig. 4. HEXIM1 represses the functional interaction between GR and TIF2. (*A*) HeLa cells were treated with 100 nM DEX or vehicle [0.1% ethanol, Tx(−)] for 1 h and subjected to indirect immunofluorescence. Confocal laser microscopic images of GR, HEXIM1, and TIF2 are shown. (*B*) COS7 cells were cotransfected with GRE-Luc and expression plasmids for GR, HEXIM1, and TIF2, as indicated. After 24 h of treatment with 100 nM DEX, whole-cell extracts were prepared and subjected to luciferase assay. (*C*) HeLa cells were infected with AdCALNL/FHhHEXIM1 (multiplicity of infection = 30) alone (Cre −) or along with recombinant adenovirus expressing Cre recombinase (Cre +). After 1 h treatment with 1 μM DEX, nuclear extracts (NE) were prepared and immunoprecipitated (IP) with anti-TIF2 antibody. Immunocomplexes were analyzed on Western blots as indicated.

cellular HEXIM1 levels may determine the sensitivity to the hormone in peripheral tissues.

It should be noted that binding of HEXIM1 to 7SK or GR is mediated by the common central arginine-rich motif. The use of the same domain or motif in recognition of nucleic acid and polypeptide molecules is often observed, and two strategies are known to achieve this type of interaction: macromolecular mimicry and induced fit mechanisms (35). The former is observed, for example, in tRNA and polypeptide release factor binding to the same domain of ribosome (36) and in TAFII230 and TATA box element DNA binding to TATA-binding protein (37). The latter is observed in interactions between RNA and arginine-rich motifs (38). The N-terminal part of the HEXIM1 NLS is almost perfectly aligned with the TAR RNA-binding motif of the HIV-1 Tat protein (10). It is known that arginine-rich motifs from different proteins adopt different conformations dependent on the RNA sites recognized and in some cases fold only in the presence of RNA (38). The formation of the Tat/TAR/P-TEFb complex in HIV-infected cells may, therefore, compete and preclude the formation of the inactive

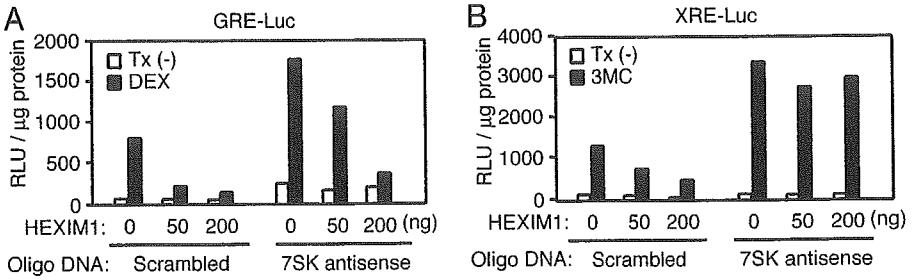

Fig. 5. P-TEFb-dependent and -independent suppression of transcription by HEXIM1. HepG2 cells were cotransfected with the xenobiotic responsive reporter plasmid XRE-Luc or GRE-Luc and indicated amounts of HEXIM1 expression plasmid, along with scrambled or 7SK antisense deoxyoligonucleotides, and treated with 1 μM 3-methylchoranthrene (3MC) or 100 nM DEX for 24 h. Whole-cell extracts were prepared and subjected to luciferase assay. Tx, treatment; RLU, relative light units.

HEXIM1/7SK/P-TEFb complex with resultant activation of the HIV-1 transcription. Because GR also targets the NLS of HEXIM1, it is extremely intriguing to speculate that HEXIM1, by differential formation of distinct protein–protein and protein–RNA complexes through its NLS, modulates cellular gene expression and host defense systems. In this line, it is of particular importance to study how HEXIM1 distinguishes GR and 7SK to form distinct modules. Along this line, continued study is necessary to compare structures of TAR/Tat, HEXIM1/7SK, and HEXIM1/GR and to understand differential roles of HEXIMs in transcriptional regulation in more detail.

In conclusion, we showed that HEXIM1, in addition to the HEXIM1/7SK/P-TEFb complex, specifically binds GR to form a transcriptionally inactive complex. Together with the results of AhR, these data suggest that this mode of complex formation may be restricted to a certain class of transcription factors including GR. HEXIM1 might serve as a molecular device to give distinct biological cues: suppression of transcriptional elongation and repression of GR-mediated transcription.

We thank H. Iba, I. Saito, and T. Wada for material transfer and helpful suggestions and discussion; M. Hasegawa and Y. Tsuboi for technical assistance in mass spectrometric analyses; and Y. Yamaguchi for critical reading of the manuscript. This work was supported in part by grants from the Ministry of Education, Science, Technology, Sports, and Culture; the Ministry of Health, Labour, and Welfare; and the Japan Society for the Promotion of Science. N.S. is a Japan Society for the Promotion of Science Research Fellow.

1. Sims, R. J., III, Mandal, S. S. & Reinberg, D. (2004) *Curr. Opin. Cell Biol.* **16,** 263–271.
2. Woychik, N. A. & Hampsey, M. (2002) *Cell* **108,** 453–463.
3. Kadonaga, J. T. (2004) *Cell* **116,** 247–257.
4. Arndt, K. M. & Kane, C. M. (2003) *Trends Genet.* **19,** 543–550.
5. Hartzog, G. A. (2003) *Curr. Opin. Genet. Dev.* **13,** 119–126.
6. Sims, R. J., III, Belotserkovskaya, R. & Reinberg, D. (2004) *Genes Dev.* **18,** 2437–2468.
7. Kusuhara, M., Nagasaki, K., Kimura, K., Maass, N., Manabe, T., Ishikawa, S., Aikawa, M., Miyazaki, K. & Yamaguchi, K. (1999) *Biomed. Res.* **20,** 273–279.
8. Ouchida, R., Kusuhara, M., Shimizu, N., Hisada, T., Makino, Y., Morimoto, C., Handa, H., Ohsuzu, F. & Tanaka, H. (2003) *Genes Cells* **8,** 95–107.
9. Michels, A. A., Nguyen, V. T., Fraldi, A., Labas, V., Edwards, M., Bonnet, F., Lania, L. & Bensaude, O. (2003) *Mol. Cell Biol.* **23,** 4859–4869.
10. Yik, J. H., Chen, R., Nishimura, R., Jennings, J. L., Link, A. J. & Zhou, Q. (2003) *Mol. Cell* **12,** 971–982.
11. Michels, A. A., Fraldi, A., Li, Q., Adamson, T. E., Bonnet, F., Nguyen, V. T., Sedore, S. C., Price, J. P., Price, D. H., Lania, L. & Bensaude, O. (2004) *EMBO J.* **23,** 2608–2619.
12. Yik, J. H., Chen, R., Pezda, A. C., Samford, C. S. & Zhou, Q. (2004) *Mol. Cell Biol.* **24,** 5094–5105.
13. Nguyen, V. T., Kiss, T., Michels, A. A. & Bensaude, O. (2001) *Nature* **414,** 322–325.
14. Yang, Z., Zhu, Q., Luo, K. & Zhou, Q. (2001) *Nature* **414,** 317–322.
15. Wittmann, B. M., Wang, N. & Montano, M. M. (2003) *Cancer Res.* **63,** 5151–5158.
16. Yik, J. H., Chen, R., Pezda, A. C. & Zhou, Q. (2005) *J. Biol. Chem.* **280,** 16368–16376.
17. Byers, S. A., Price, J. P., Cooper, J. J., Li, Q. & Price, D. H. (2005) *J. Biol. Chem.* **280,** 16360–16367.
18. Beato, M., Herrlich, P. & Schutz, G. (1995) *Cell* **83,** 851–857.
19. Mangelsdorf, D. J., Thummel, C., Beato, M., Herrlich, P., Schutz, G., Umesono, K., Blumberg, B., Kastner, P., Mark, M., Chambon, P., *et al.* (1995) *Cell* **83,** 835–839.
20. Perlmann, T., Rangarajan, P. N., Umesono, K. & Evans, R. M. (1993) *Genes Dev.* **7,** 1411–1422.
21. Yoshikawa, N., Makino, Y., Okamoto, K., Morimoto, C., Makino, I. & Tanaka, H. (2002) *J. Biol. Chem.* **277,** 5529–5540.
22. Kodama, T., Shimizu, N., Yoshikawa, N., Makino, Y., Ouchida, R., Okamoto, K., Hisada, T., Nakamura, H., Morimoto, C. & Tanaka, H. (2003) *J. Biol. Chem.* **278,** 33384–33391.
23. Shimizu, N., Sugimoto, K., Tang, J., Nishi, T., Sato, I., Hiramoto, M., Aizawa, S., Hatakeyama, M., Ohba, R., Hatori, H., *et al.* (2000) *Nat. Biotechnol.* **18,** 877–881.
24. Nishi, T., Shimizu, N., Hiramoto, M., Sato, I., Yamaguchi, Y., Hasegawa, M., Aizawa, S., Tanaka, H., Kataoka, K., Watanabe, H. & Handa, H. (2002) *J. Biol. Chem.* **277,** 44548–44556.
25. Yoshikawa, N., Yamamoto, K., Shimizu, N., Yamada, S., Morimoto, C. & Tanaka, H. (2005) *Mol. Endocrinol.* **19,** 1110–1124.
26. Hiramoto, M., Shimizu, N., Sugimoto, K., Tang, J., Kawakami, Y., Ito, M., Aizawa, S., Tanaka, H., Makino, I. & Handa, H. (1998) *J. Immunol.* **160,** 810–819.
27. Harmer, D., Gilbert, M., Borman, R. & Clark, K. L. (2002) *FEBS Lett.* **532,** 107–110.
28. Duester, G., Farres, J., Felder, M. R., Holmes, R. S., Hoog, J. O., Pares, X., Plapp, B. V., Yin, S. J. & Jornvall, H. (1999) *Biochem. Pharmacol.* **58,** 389–395.
29. Kobayashi, T., Deak, M., Morrice, N. & Cohen, P. (1999) *Biochem. J.* **344 Pt 1,** 189–197.
30. Watanabe, H., Suzuki, A., Goto, M., Ohsako, S., Tohyama, C., Handa, H. & Iguchi, T. (2004) *J. Mol. Endocrinol.* **33,** 763–771.
31. Tian, Y., Ke, S., Chen, M. & Sheng, T. (2003) *J. Biol. Chem.* **278,** 44041–44048.
32. Beischlag, T. V., Wang, S., Rose, D. W., Torchia, J., Reisz-Porszasz, S., Muhammad, K., Nelson, W. E., Probst, M. R., Rosenfeld, M. G. & Hankinson, O. (2002) *Mol. Cell Biol.* **22,** 4319–4333.
33. Huang, F., Wagner, M. & Siddiqui, M. A. (2004) *Mech. Dev.* **121,** 559–572.
34. Sano, M., Abdellatif, M., Oh, H., Xie, M., Bagella, L., Giordano, A., Michael, L. H., DeMayo, F. J. & Schneider, M. D. (2002) *Nat. Med.* **8,** 1310–1317.
35. Nissen, P., Kjeldgaard, M. & Nyborg, J. (2000) *EMBO J.* **19,** 489–495.
36. Song, H., Mugnier, P., Das, A. K., Webb, H. M., Evans, D. R., Tuite, M. F., Hemmings, B. A. & Barford, D. (2000) *Cell* **100,** 311–321.
37. Liu, D., Ishima, R., Tong, K. I., Bagby, S., Kokubo, T., Muhandiram, D. R., Kay, L. E., Nakatani, Y. & Ikura, M. (1998) *Cell* **94,** 573–583.
38. Smith, C. A., Calabro, V. & Frankel, A. D. (2000) *Mol. Cell* **6,** 1067–1076.

CD26 Regulates p38 Mitogen-Activated Protein Kinase–Dependent Phosphorylation of Integrin β_1, Adhesion to Extracellular Matrix, and Tumorigenicity of T-Anaplastic Large Cell Lymphoma Karpas 299

Tsutomu Sato,[1] Tadanori Yamochi,[1] Toshiko Yamochi,[1] Ugur Aytac,[1] Kei Ohnuma,[2] Kathryn S. McKee,[1] Chikao Morimoto,[2] and Nam H. Dang[1]

[1]Department of Lymphoma/Myeloma, University of Texas M.D. Anderson Cancer Center, Houston, Texas and [2]Department of Clinical Immunology, Institute of Medical Science, University of Tokyo, Tokyo, Japan

Abstract

CD26 is an antigen with key role in T-cell biology and is expressed on selected subsets of aggressive T-cell malignancies. To elucidate the role of CD26 in tumor behavior, we examine the effect of CD26 depletion by small interfering RNA transfection of T-anaplastic large cell lymphoma Karpas 299. We show that the resultant CD26-depleted clones lose the ability to adhere to fibronectin and collagen I. Because anti-integrin β_1 blocking antibodies also prevent binding of Karpas 299 to fibronectin and collagen I, we then evaluate the CD26-integrin β_1 association. CD26 depletion does not decrease integrin β_1 expression but leads to dephosphorylation of both integrin β_1 and p38 mitogen-activated protein kinase (MAPK). Moreover, our data showing that the p38MAPK inhibitor SB203580 dephosphorylates integrin β_1 and that binding of the anti-CD26 antibody 202.36 dephosphorylates both p38MAPK and integrin β_1 on Karpas 299, leading to loss of cell adhesion to the extracellular matrix, indicate that CD26 mediates cell adhesion through p38MAPK-dependent phosphorylation of integrin β_1. Finally, *in vivo* experiments show that depletion of CD26 is associated with loss of tumorigenicity and greater survival. Our findings hence suggest that CD26 plays an important role in tumor development and may be a novel therapeutic target for selected neoplasms. (Cancer Res 2005; 65(15): 6950-6)

Introduction

CD26/dipeptidyl peptidase IV is a 110-kDa cell surface glycoprotein that belongs to the serine protease family and is expressed on a variety of tissues, including T lymphocytes, endothelial cells, and epithelial cells. It is composed of a short cytoplasmic domain, a transmembrane region, and an extracellular domain with dipeptidyl peptidase IV activity, which selectively removes the NH_2-terminal dipeptide from polypeptides containing either a proline or an alanine at the penultimate residue. This enzymatic activity seems to regulate the effect of several crucial cytokines and chemokines (1). Work over the past decade has shown CD26 to have an important role in T-cell biology both as a marker of T-cell activation and as a structure associated with key molecules and signaling pathways (2–5).

Requests for reprints: Nam H. Dang, Department of Hematologic Oncology, Nevada Cancer Institute, 10000 West Charleston Boulevard, Suite 260, Las Vegas, NV 89135. Phone: 702-821-0000; Fax: 702-821-0021; E-mail: ndang@nvcancer.org.

Although the role of CD26 in the regulation of normal T-cell physiology has been well characterized, its involvement in tumor biology is still unclear, although early data suggested that it may have a role in the development of selected neoplasms. Studies of patient samples showed that CD26 is highly expressed on lung adenocarcinoma, thyroid carcinoma, and B-cell chronic lymphocytic leukemia (6–8). Meanwhile, CD26 is a marker of aggressive disease for selected subsets of T-cell non-Hodgkin's lymphomas/leukemias. Carbone et al. showed that CD26 expression is restricted to such aggressive types of T-cell malignancies as T-lymphoblastic lymphomas (T-LBL), T-acute lymphoblastic leukemias (T-ALL), and T-anaplastic large cell lymphomas (T-ALCL). Furthermore, multivariate analysis indicated that the expression of CD26 on T-LBL/T-ALL tumor cells is associated with a worse outcome compared with CD26-negative T-LBL/T-ALL tumors (9). Similarly, we showed recently that CD26 expression is a marker of poor prognosis for T-large granular lymphocyte lymphoproliferative disorder (10). Although these findings suggested that CD26 may regulate the malignant behavior of selected tumors, the exact mechanisms involved in the role of CD26 in tumor biology remain to be elucidated.

In this article, we evaluate the role of CD26 in tumor biology by depleting the expression of CD26 on the T-ALCL cell line Karpas 299 with the small interfering RNA (siRNA) technique. We show that CD26 mediates cell adhesion to the extracellular matrix (ECM) proteins fibronectin and collagen I through p38 mitogen-activated protein kinase (MAPK)–dependent phosphorylation of integrin β_1. We also show that CD26 expression regulates topoisomerase IIα level and tumor sensitivity to the topoisomerase II inhibitor doxorubicin. Importantly, loss of CD26 expression on Karpas 299 cells results in decreased tumorigenicity and improved survival in a severe combined immunodeficient (SCID) mouse animal model, hence suggesting that targeting CD26 may be an effective therapeutic approach for selected CD26-positive T-cell malignancies.

Materials and Methods

Reagents. All culture plates and dishes were purchased from Falcon Plastics (Oxnard, CA). Mouse anti-integrin β_1 antibody (P4C10) was from Chemicon (Temecula, CA). Mouse anti-integrin β_1 antibody (4B4) and isotypic control mouse IgG were from Beckman Coulter (Miami, FL). Mouse anti-CD26 antibody (202.36) was from Santa Cruz (Santa Cruz, CA). Mouse anti-CD26 antibodies (1F7 and 5F8) were prepared as described previously (11). Specific inhibitors against p38MAPK SB203580 was from Biomol (Plymouth, Meeting, PA). 3-(4,5-Dimethylthiazol-2-yl)-2,5-diphenyltetrazolium bromide (MTT) was from Sigma (St. Louis, MO). Doxorubicin was from Calbiochem (La Jolla, CA).

Cell culture. The human T-ALCL cell line Karpas 299 was supplied by American Type Culture Collection (Manassas, VA) and maintained in RPMI 1640 (Sigma) with 10% heat-inactivated FCS (Sigma) and antibiotics (100 IU/mL penicillin and 100 μg/mL streptomycin) at 37°C in a humidified atmosphere containing 5% CO_2.

Depletion of CD26. The expression of CD26 was suppressed by Knockout RNAi System (Clontech, Palo Alto, CA) as described previously (12). Briefly, the target sequence ATCATGCATGCAATCAAC, which corresponds to the nucleotide sequence from 1,768 to 1,785 of CD26 cDNA (accession no. NM_001935), was first determined using siDESIGN program at Dharmacon siDESIGN Center (http://design.dharmacon.com/). Complementary oligonucleotides encoding siRNA were then designed and ligated into vector RNAi-Ready pSIREN-RetroQ (Clontech) according to the manufacturer's instructions. Oligonucleotides encoding missense siRNA, in which the target sequence was replaced with the missense sequence ATC*T*TGCA*A*GCAA*A*CAAC, were also ligated into the vector as controls. For the retroviral packaging, these constructs were cotransfected with p10A1 (Clontech) into GP2-293 cells (Clontech) using LipofectAMINE reagent (Invitrogen, Carlsbad, CA). The supernatants containing retrovirus were collected 72 hours after the transfection. Then, this supernatant was added to culture medium of Karpas 299 cells, which was supplemented with 8 μg/mL polybrene (Sigma). After 3 days of incubation, the cells were cultured with 0.4 μg/mL puromycin (Clontech) to eliminate nontransfected cells. Isolated clones were obtained by the standard limiting dilution method.

3-(4,5-Dimethylthiazol-2-yl)-2,5-diphenyltetrazolium bromideassay. The cells were cultured with 100 or 300 μL medium in each well of a 96- or 24-well plate, respectively. To quantify the total number of cells, a quarter volume of the MTT solution, PBS containing 5 mg/mL MTT, was added to the culture medium. To quantify the number of adhesive cells, the culture medium, in which nonadhesive cells were floating after the plates were shaken orbitally several times, was discarded. Then, the same volume of fresh medium with a quarter volume of MTT solution was added to the remaining adhesive cells. In both quantifications, the cells were cultured for 2 hours and added with the same volume of lysis buffer as described previously (13). After overnight incubation at 37°C, the absorbance of dissolved blue formazan was measured at 570 nm in spectrophotometer μQuant (Bio-Tek, Winooski, VT) with KC junior software.

Flow cytometry. The cells were collected, washed twice with PBS, and resuspended in 0.5 mL fluorescence-activated cell sorting buffer, PBS containing 0.5 mmol/L EDTA and 1% (w/v) bovine serum albumin (Sigma). Then, the cells were incubated on ice for 30 minutes with anti-CD26 (Caltag, Burlingame, CA) or anti-integrin β_1 (4B4) mouse monoclonal antibody. Isotypic mouse IgG was used as a control. Surface antigens detected by these antibodies were visualized with FITC-conjugated anti-mouse IgG antibody (Pierce, Rockford, IL), followed by the use of FACSCalibur (Becton Dickinson, San Jose, CA) with CellQuest software.

Western blotting. Cells (1×10^7) were collected, washed twice with PBS, and resuspended in 0.3 mL lysis buffer [1% SDS, 10 mmol/L Tris-HCl (pH 7.4), 10 μg/mL leupeptin, 10 μg/mL aprotinin, 2 mmol/L phenylmethylsulfonyl fluoride] and then boiled for 5 minutes. After passage through a 20-gauge needle 10 times and centrifugation at 15,000 rpm for 20 minutes, the aliquot was boiled again with a standard 4× SDS loading buffer containing 15% (v/v) 2-mercaptoethanol for 5 minutes; 10 μL of which were then subjected to SDS-polyacrylamide gel for electrophoresis followed by the transfer to Immobilon membrane (Millipore, Bedford, MA). The membrane was hybridized with goat anti-CD26/dipeptidyl peptidase IV (R&D, Minneapolis, MN), mouse anti-topoisomerase IIα (Ki-S1, Chemicon), mouse anti-phosphotopoisomerase IIα Thr^{1342} (3D4, MBL, Nagoya Japan), goat anti-integrin β_1 L-16 (Santa Cruz), rabbit anti-integrin β_1 $pSer^{785}$ (Biosource, Camarillo, CA), rabbit anti-p38MAPK (Cell Signaling, Beverly, MA), or rabbit anti-phospho-p38MAPK Thr^{180}/Tyr^{182} (Cell Signaling) antibodies. Proteins detected by these antibodies were visualized with horseradish peroxidase–conjugated anti-mouse (DAKOCytomation, Kyoto, Japan), rabbit (Bio-Rad, Hercules, CA), or goat (DAKOCytomation) antibody followed by the use of SuperSignal West Pico Stable Peroxidase Solution (Pierce).

***In vivo* experiments.** Three-week-old female CB-17 SCID mice were purchased from Taconic Farms (Germantown, NY). The mice were kept in laminar flow rooms at constant temperature and humidity. They had free access to food and water. Experimental protocols were approved by the Institutional Ethics Committee for Animal Experimentation. Briefly, every

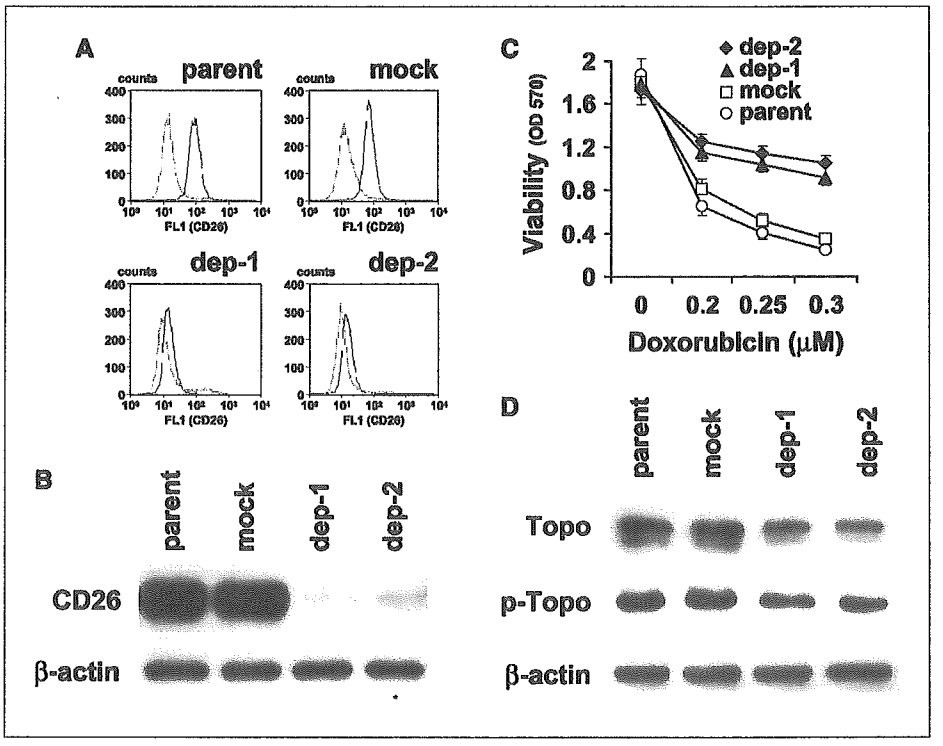

Figure 1. Effect of CD26 depletion on topoisomerase IIα expression and sensitivity to doxorubicin. Karpas 299 cells (parent) were retrovirally transfected with siRNA against CD26. The clones selected by the standard limiting dilution method were designated CD26-depleted clone 1 (dep-1) and clone 2 (dep-2). The control was a clone transfected with missense siRNA (mock). The expression of CD26 was examined by flow cytometry (*A*) and Western blotting (*B*). *A,solid lines* or *broken lines*, cells treated with anti-CD26 antibody or isotype control IgG, respectively. *B*, equal amount of proteins was loaded in each lane, with β-actin as control. *C*, Karpas 299 cells (parent, ○), mock (□), and CD26-depleted clones (dep-1, ▲; dep-2, ◆) were plated onto 96-well culture plate (2×10^4 cells per well) and cultured with the indicated concentrations of doxorubicin for 3 days. Following the incubation period, the number of total cell was quantified by MTT assay as described in Materials and Methods. *Points*, mean of five separate experiments ($n = 5$); *bars*, SD. *D*, topoisomerase IIα (*Topo*) and phosphorylated topoisomerase IIα at Thr^{1342} (*p-Topo*) of Karpas 299 cells (parent), mock, and CD26-depleted clones (dep-1 and dep-2) were evaluated by Western blotting as described in Materials and Methods, with each lane being loaded with equal amount of proteins and with β-actin as control.

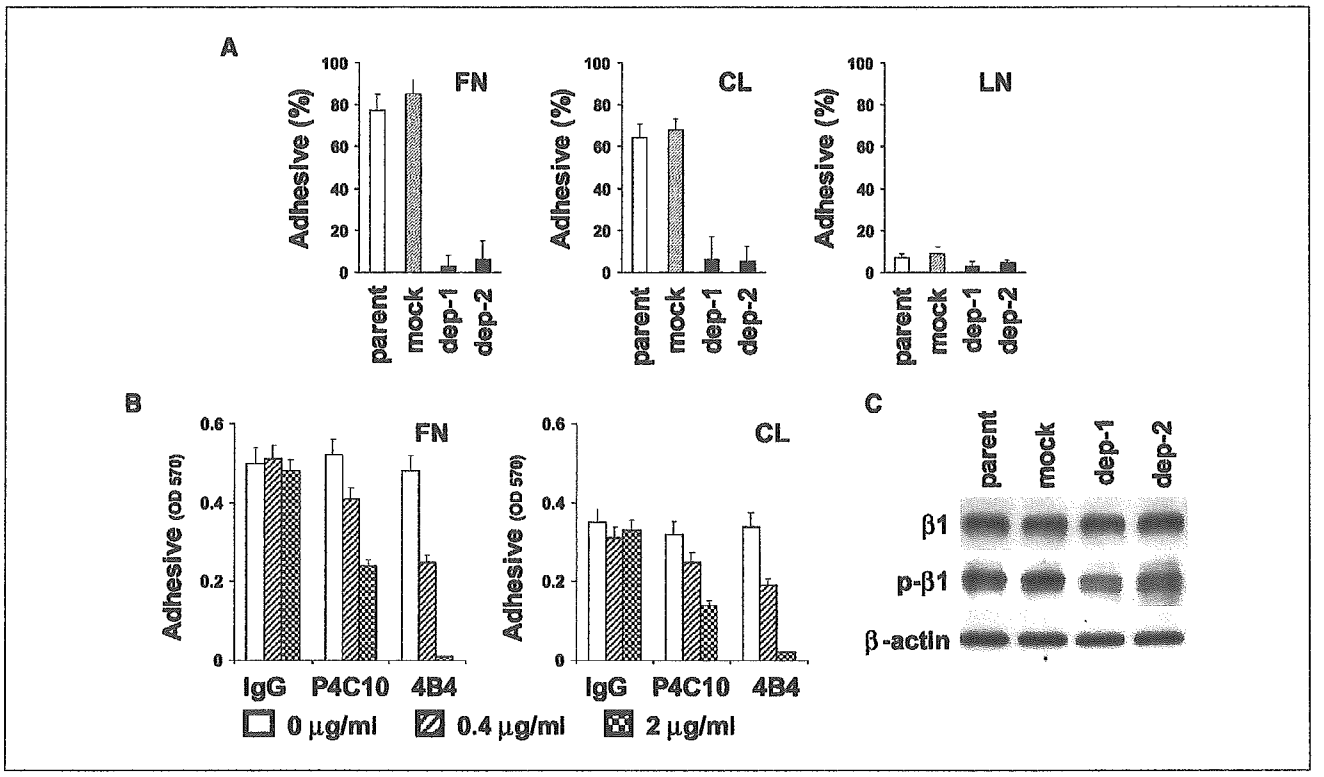

Figure 2. Effect of CD26 depletion on cell adhesion to ECM and integrin β_1 phosphorylation. *A*, Karpas 299 cells (parent; *open columns*), mock (*shaded columns*), and CD26-depleted clones (dep-1 and dep-2; *closed columns*) were plated onto 60 mm dishes (3×10^6 cells per dish) coated with fibronectin (*FN*), collagen I (*CL*), or laminin (*LN*) and cultured for 3 hours. Then, nonadhesive and adhesive cells were separately collected and counted using a hemocytometer. Adhesive cells (%): adhesive cells / adhesive cells + nonadhesive cells. *Columns,* mean of five separate experiments ($n = 5$); *bars,* SD. *B,* Karpas 299 cells were preincubated with 0 (*open columns*), 0.4 (*shaded columns*), or 2 (*hatched columns*) μg/mL blocking antibodies against integrin β_1 (P4C10 or 4B4) for 30 minutes at room temperature. The cells were then plated onto 24-well plates (3×10^5 cells per well) coated with fibronectin or collagen I and placed at room temperature for 1 hour. Following washing of plates to discard nonadhesive cells, the number of adhesive cells remaining was then quantified by MTT assay as described in Materials and Methods. Cells preincubated with isotype control IgG were used as control. *Columns,* mean of five separate experiments ($n = 5$); *bars,* SD. *C,* expression of integrin β_1 (*β1*) and phosphorylated integrin β_1 at Ser^{785} (*p-β1*) on Karpas 299 cells (parent), mock, and CD26-depleted clones (dep-1 and dep-2) was examined by Western blotting as described in Materials and Methods, with equal amount of proteins being loaded in each lane and with β-actin as control.

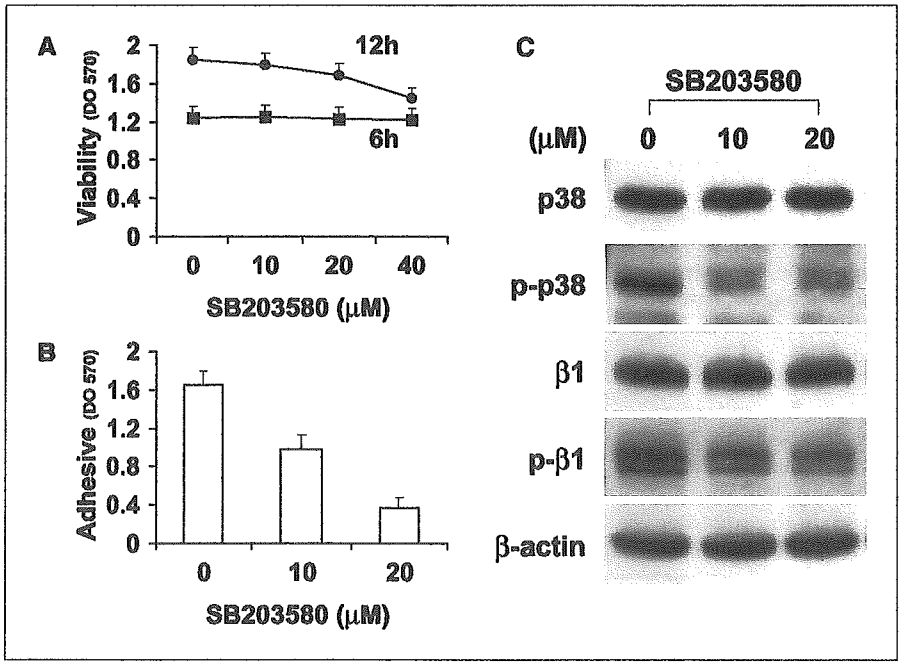

Figure 3. Effect of the p38MAPK inhibitor SB203580 on integrin β_1 phosphorylation. Karpas 299 cells were initially cultured in 24-well plates (3×10^5 cells per well; *A* and *B*) or 10 cm dish (1×10^7 cells per dish; *C*) coated with fibronectin for 6 hours. The cells were then incubated with the indicated concentrations of the p38MAPK inhibitor SB203580 dissolved in DMSO. A final DMSO concentration of 0.4% (v/v) was achieved equally in all samples. *A,* following incubation with SB203580 at 6 (■) or 12 (●) hours, MTT assays were then done as described in Materials and Methods to determine cell viability. *Points,* mean of five separate experiments ($n = 5$); *bars,* SD. *B,* following incubation with SB203580 at 6 hours, plates were washed to discard nonadhesive cells and the number of adhesive cells remaining was quantified by MTT assay as described in Materials and Methods. *Columns,* mean of five separate experiments ($n = 5$); *bars,* SD. *C,* following incubation with SB203580 at 6 hours, levels of p38MAPK (*p38*), phosphorylated p38MAPK at Thr^{180}/Tyr^{182} (*p-p38*), integrin β_1, and phosphorylated integrin β_1 at Ser^{785} were evaluated by Western blotting as described in Materials and Methods, with each lane being loaded with equal amount of proteins and with β-actin as control.

mouse has received i.p. injection of 0.2 mL rabbit anti-asialo-GM1 antisera (Wako Pure Chemical, Osaka, Japan) on day −1. The mice were subsequently divided into three groups, each of which included five animals. Every mouse in each group was then injected i.p. with 0.3×10^6 cells of mock or CD26-depleted clones (dep-1 and dep-2) on day 0. The growth of the palpable tumor in the inguinal regions was followed by measurements with a caliper and its volume was calculated according to the following formula: $MD \times TL^2 \times 1/2$, where MD and TL are the maximum diameter and transverse length, respectively. The mice were sacrificed before the volume of the tumor mass reached 3,000 mm^3 for ethical reason.

Results

Transfection of small interfering RNA against CD26 depletes its expression on Karpas 299 cells. Because CD26 surface expression is associated with aggressive disease in certain types of T-cell malignancies, including T-ALCL (9, 14), we evaluated the role of CD26 in the T-ALCL cell line Karpas 299, which expresses high level of CD26. To deplete CD26 expression, Karpas 299 cells (parent) were retrovirally transfected with siRNA against CD26. Two permanent transfectants were subsequently obtained and designated as CD26-depleted clone 1 (dep-1) and clone 2 (dep-2). The cells transfected with missense siRNA were used as controls (mock). Flow cytometry studies (Fig. 1*A*) and Western blotting analyses (Fig. 1*B*) indicate that CD26 expression is almost completely abrogated on CD26-depleted clones.

CD26 depletion is associated with decreased topoisomerase IIα level and decreased sensitivity to doxorubicin. We showed previously that transfectional overexpression of CD26 results in the up-regulation of topoisomerase IIα expression, associated with enhanced sensitivity to the topoisomerase II inhibitor doxorubicin (12, 15–17). Consistent with our earlier work, our present studies clearly show that CD26 depletion results in decreased doxorubicin sensitivity (Fig. 1*C*). Furthermore, we found that the expression of topoisomerase IIα as well as its phosphorylated active form (18) is down-regulated in CD26-depleted clones (Fig. 1*D*). In contrast, the expression of other structures associated with doxorubicin sensitivity, such as lung resistance protein, multidrug resistance protein-1, and P-glycoprotein, is not influenced by CD26 depletion (data not shown).

CD26 regulates cell adhesion to extracellular matrix through phosphorylation of integrin β_1. CD26 has been described previously to play a role in cell adhesion to the ECM under certain experimental conditions (1, 19). Evaluating the potential effect of CD26 on tumor binding to the ECM, we found that parental Karpas 299 cells and mock clone display greater adhesion to the ECM proteins fibronectin and type I collagen I than CD26-depleted clones (Fig. 2*A*). Because integrins have a well-established role in cell adhesion to ECM proteins, we evaluated the potential association between CD26 and integrin β_1, which is involved in cell adhesion to both fibronectin and collagen I (20). We found that anti-integrin β_1 antibodies significantly block the adhesion of Karpas 299 cells to both fibronectin and collagen I as shown in Fig. 2*B*. Examining further the association between CD26 expression and integrin β_1-dependent cell adhesion, we found no difference in the expression level of integrin β_1 among parental Karpas 299 cells, mock cells, and CD26-depleted clones by flow cytometry (data not shown) and Western blotting (Fig. 2*C*). We next focused on the level of phosphorylated integrin β_1 at residue Ser^{785}, which is necessary for integrin β_1 to function as an adhesion molecule (21). Our findings showed that there is lower level of phosphorylation at integrin β_1 Ser^{785} in CD26-depleted clones than in parental Karpas 299 and mock cells (Fig. 2*C*).

p38MAPK intermediates between CD26 and integrin β_1. We reported recently an association between CD26 and p38MAPK, with overexpression of CD26 resulting in increased p38 phosphorylation at Thr^{180}/Tyr^{182} and depletion of CD26 level leading to decreased p38 phosphorylation at the same residues (12). We therefore examined the possible relationship between p38MAPK and integrin β_1 using the p38MAPK-specific inhibitor SB203580. Although incubation of Karpas 299 cells with SB203580 for 6 hours up to a concentration of 40 μmol/L (Fig. 3*A*) does not lead to decreased cell viability, there is a dose-dependent inhibition of cell adhesion (Fig. 3*B*). In addition, treatment with SB203580 is accompanied by a gradual dephosphorylation of integrin β_1 at Ser^{785} as well as p38MAPK at Thr^{180}/Tyr^{182} (Fig. 3*C*).

Anti-CD26 antibody 202.36 inhibits cell adhesion with dephosphorylation of p38MAPK and integrin β_1. To further delineate CD26 association with p38MAPK and integrin β_1, we

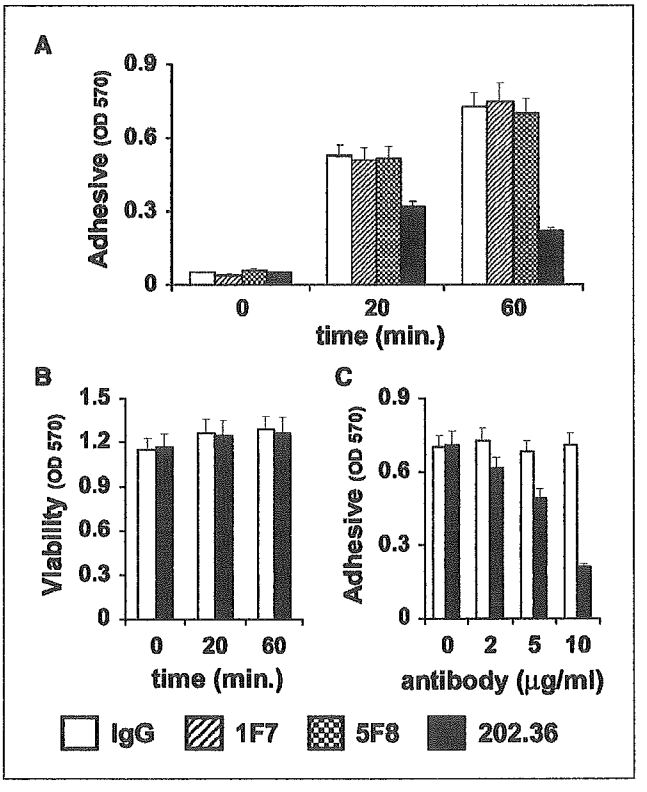

Figure 4. Effect of the anti-CD26 antibody 202.36 on adhesion of Karpas 299 cells to ECM. *A*, Karpas 299 cells were plated onto 24-well plates (3×10^5 cells per well) coated with fibronectin. Shortly thereafter, each antibody (10 μg/mL) was added and the cells were incubated for the indicated times. *Open*, *shaded*, *hatched*, or *closed columns*, isotype control IgG or anti-CD26 antibody clone 1F7, 5F8, or 202.36, respectively. After the incubation period, plates were washed to discard nonadhesive cells and the number of adhesive cells remaining was then quantified by MTT assay as described in Materials and Methods. *B*, cells were treated with 10 μg/mL IgG or 202.36 and incubated for the indicated times. After the incubation period, MTT assays were then done as described in Materials and Methods to determine cell viability. *C*, cells were treated with the indicated concentrations of IgG or 202.36 and incubated for 60 minutes. After the incubation time, plates were washed to discard nonadhesive cells and the number of adhesive cells remaining was then quantified by MTT assay as described in Materials and Methods. *Columns*, mean of five separate experiments ($n = 5$); *bars*, SD (*A-C*).